Observations of Decadal-Scale Brine Chemistry Change at the Bonneville Salt Flats, Utah

Jeremiah A. Bernau[1,2], Brenda B. Bowen[1], Evan L. Kipnis[1], and Jory C. Lerback[1,3]

[1]Department of Geology and Geophysics, University of Utah, Salt Lake City, Utah, jeremiahbernau@gmail.com
[2]Utah Geological Survey, Salt Lake City, Utah
[3]Department of Earth, Planetary and Space Sciences, University of California, Los Angeles, California

ABSTRACT

Over the past century, the Bonneville Salt Flats, which lies on the western edge of the Great Salt Lake watershed, has experienced changing environmental conditions and a unique history of land use, including resource extraction and recreation. The perennial halite salt crust has decreased in thickness since at least 1960. An experimental restoration project to return mined solutes began in 1997, but it has not resulted in anticipated salt crust growth. Here, primary observations of the Bonneville Salt Flats surface and subsurface brine chemistry and water levels collected from 2013 to 2023 are reported. Spatial and temporal patterns in chemistry, focused on density and water stable isotopes, are evaluated and compared with observations across seven periods of research spanning from 1925 to 2023. Declining salinity in the areas to the east of extraction ditches and south of Interstate 80 were observed. Brine extracted for potash production decreased in salinity as extraction rates increased. Between the years 1964 and 1997, brine in the shallow aquifer located beneath and to the east of the crust experienced a decrease in salinity. However, following this period, the salinity stabilized and subsequently increased. Salinity recovery was concurrent with declines in brine extraction and the salt restoration project, with the largest decrease in brine extraction being concurrent with the largest recovery in salinity. The specific impact of the restoration project on the brine salinity increase remains unclear. To the west, the shallow aquifer in the area between the Silver Island Mountains and the salt crust has increased in salinity. This increase is accompanied by a decline in groundwater levels, which enables the underground movement of solutes from east to west, following a salinity gradient away from the saline pan. Over the past 25 years, water levels in the alluvial-fan aquifer along the Silver Island Mountains have markedly declined, leading to the extraction of increasingly more saline and isotopically heavier basinal waters are intriguing landscapes for industrial use. This change is concurrent with the onset of the salt restoration project, which relies on alluvial-fan aquifer waters. This article's compilation of changes in groundwater chemistry provides an important resource for stakeholders working to understand and manage this dynamic and ephemeral evaporite system. It also offers an example of decadal-scale change in a highly managed Great Salt Lake watershed saline system.

INTRODUCTION

Saline pans, shallow depressions encrusted by evaporites where waters accumulate, provide an intriguing example where groundwater level and chemistry, climate, and anthropogenic activities converge. Here, several decades of chemical measurements, with a focus on density, are used to examine how the Bonneville Salt Flats (BSF) groundwater system changed in response to: 1) brine extraction for potash production, 2) alluvial-fan groundwater extraction for industrial uses, and 3) 25 years of an experimental brine "laydown" program to restore the saline pan (Figures 1 to 3) (Kipnis and Bowen, 2018). The laydown program uses alluvial-fan aquifer groundwater to dissolve the potash mine's halite (NaCl) by-product and transport it to the saline pan in hopes of restoring saline pan thickness and extent. Multi-

decadal analyses of satellite imagery and reoccurring measurements of salt crust thickness show long-term declines in crust thickness and extent (Bowen and others, 2017; Bowen and others, 2018; Radwin and Bowen, 2021). One-third of the crust consists of halite (NaCl) and two-thirds of it is gypsum ($CaSO_4 \cdot 2H_2O$). The multi-decadal nature of research on BSF and the uniquely involved mix of stakeholders including racing enthusiasts, recreational visitors, the potash industry, researchers, and governmental managers make this site well-suited for examining the evolution of brine chemistry. This landscape is dynamic with seasonal to decadal-scale changes in flooding and saline pan volume (Figure 2E and F) (Bowen and others, 2017). Here, this examination of long-term changes in brine chemistry, with groundwater levels as a secondary dataset, provides context for the relative impact of extraction and restoration
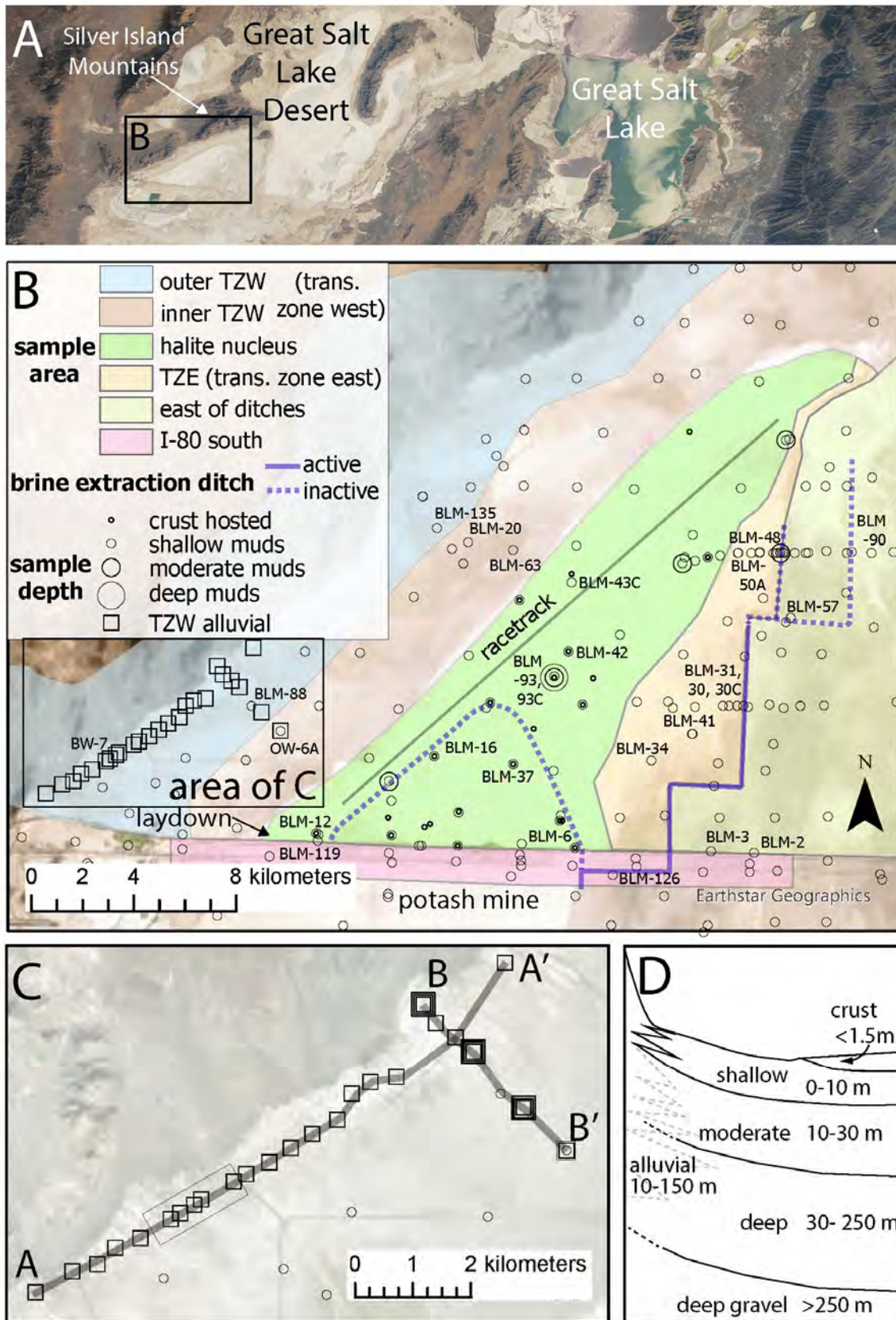
Figure 1. Site overview. A. Off-angle International Space Station image of Bonneville Salt Flats, Great Salt Lake Desert, and Great Salt Lake (https://earthobservatory.nasa.gov/images/91765/bonneville-salt-flats). B) Areas of investigation. Sample areas (divided as zones moving east from west) and depths of different sampling wells noted in figure explanation. Inset C) shows locations of brackish water (BW) alluvial-fan aquifer production wells (A-A') and nested observational wells (OW) (B-B') along transects. Primary production wells outlined by box in the middle of A-A'. D) Schematic of investigated aquifer intervals (not to scale). Basemap imagery from Earthstar Geographics.
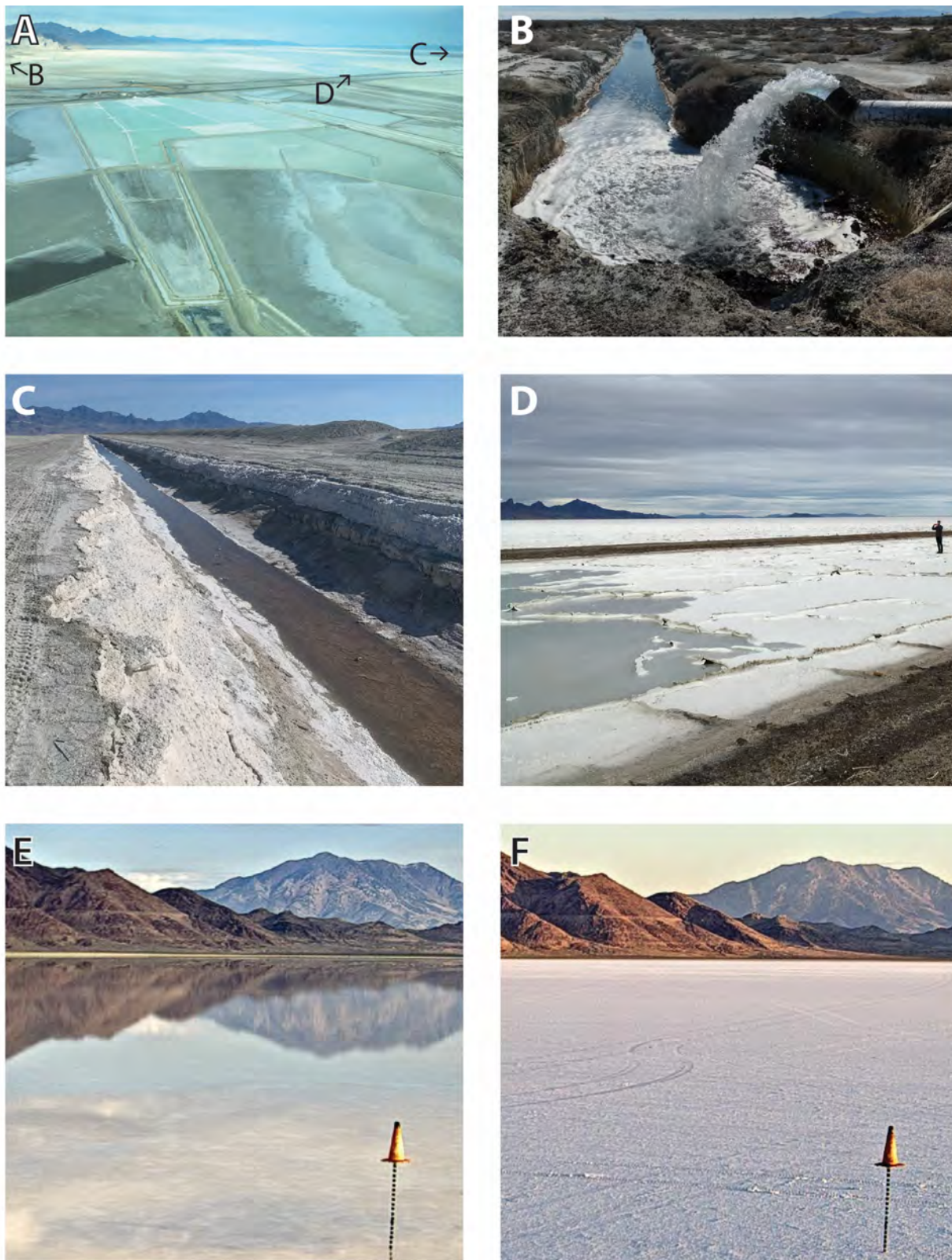
Figure 2. *Features influencing brine density and surface variation at BSF. A). Aerial photograph of potash mine looking north to BSF, letters denote relative locations of B to D. B) Alluvial-fan aquifer wells collect brackish water that is used in mine operations and to create salt laydown. C) Brine collection ditch (6 m deep) (Bingham, 1980) east of BSF (looking north). D) Laydown brine being introduced to BSF's southwest corner, person on right for scale. E and F) Time-lapse photos from BSF weather station on E) May 28, 2018, when the surface was flooded, and F) July 15, 2018, when the surface was desiccated. More field and aerial imagery of BSF is available with t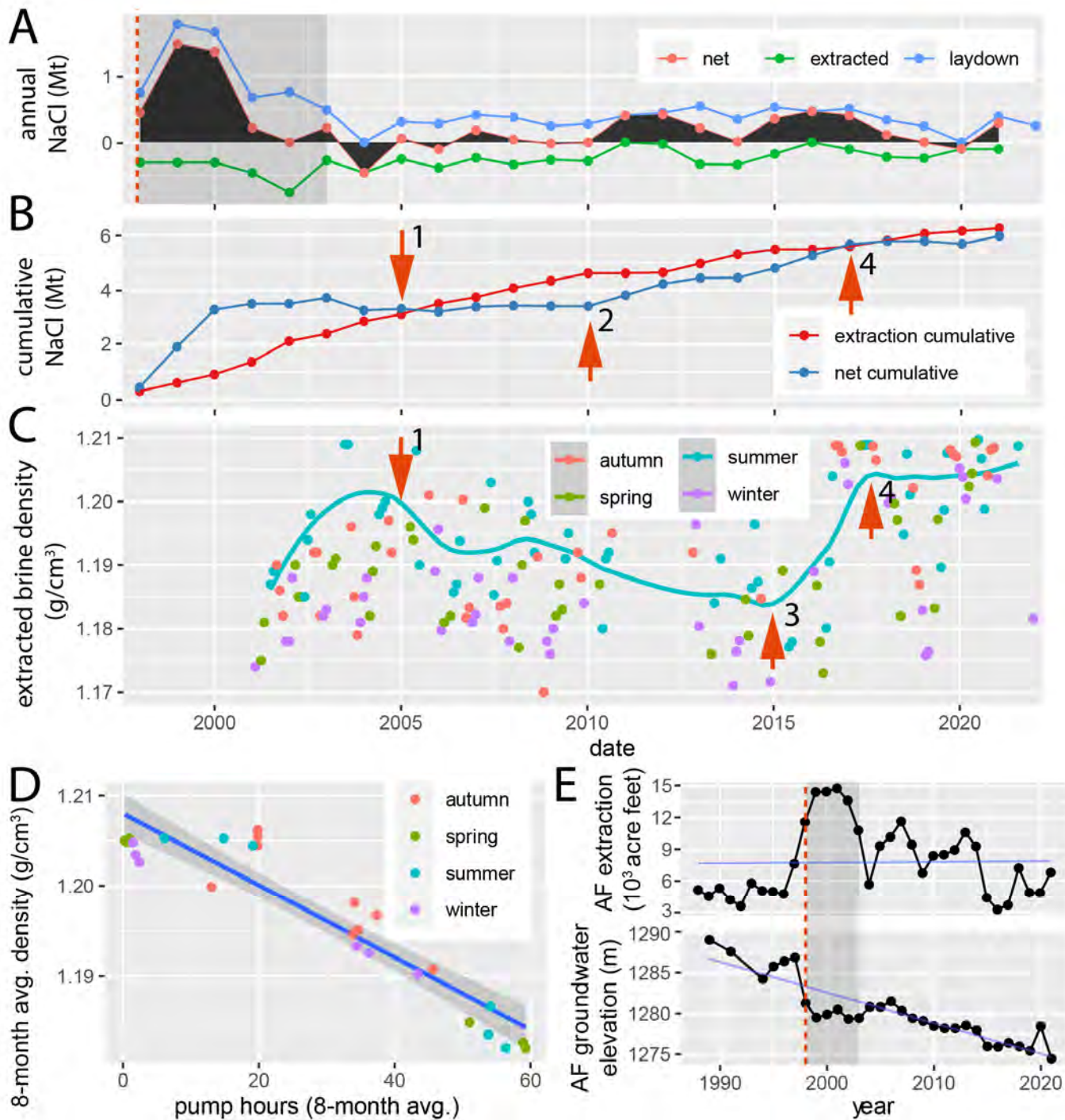he Utah Geological Survey Data Archive system at https://geodata.geology.utah.gov/pages/search.php?search=%21collection129324.*

Figure 3. *Human activities (mining and laydown) that impact brine and solute mass through time. Changes in brine mass balance (A and B) in millions of tonnes (Mt) of NaCl (not brine), the density of extracted brines (C and D), and alluvial-fan aquifer (AF) groundwater extraction and groundwater levels (E). A) Annual values NaCl mass extracted from BSF's western ditches, added to the saline pan through the laydown, and net annual NaCl balance. B) Cumulative net movement of NaCl onto BSF from the laydown. C) Changes in extracted brine salinity over time. Note seasonality in density; summer values used for long-term trend. Numbered red arrows added to B) and C) highlight notable inflection points in data. In 2006 (point 1) the salinity of extracted brine began a long-term decline. Net cumulative brine contributions were neutral between 2005 and 2010 (point 2), and increased afterward; despite this increase, extracted brines did not begin to recover in salinity until 2015 (point 3). After 2017 (point 4) extracted brine salinity remains relatively high, while extraction is low. D) Correlation between pumping and extracted brine salinity (each dot represents the average of 8 months of pumping and brine density values) from Aug. 2018 to Dec. 2020 (these values are reported as hours of pumping, ~0.85 acre-ft/hour). E) Alluvial-fan annual groundwater extraction and groundwater elevation (meters above sea level) change over time (well located at 2.3 km in Figure 12) (10^3 acre-ft ≈ $1.23*10^6$ m^3). The vertical dashed red line shows when laydown began, and the gray area on (A) and (D) emphasizes the period with elevated laydown volumes and lower than anticipated (light blue line in lower E) groundwater levels. Alluvial-fan extraction data from https://www.waterrights.utah.gov/cgi-bin/wuseview.exe?Modinfo=WRUseage&wrnum=16-25.*

activities on changing saline pan extent and volume (Figure 3). This improved knowledge will help guide plans to optimize the sustained use, including both mining and racing, of this landscape.

METHODS

Brine chemistry was characterized and groundwater levels were measured at BSF between 2015 and 2023. Measurements prior to 2015 were compiled. This study involved extensive density measurement quality control, analyzing trends in individual wells, and analyzing data aggregated by area and aquifer. Here, groundwater levels are reported to provide context for observed changes; however, they are not the primary focus of this work.

Data Sources Over Time

Groundwater level and density data were divided over seven study periods that vary in length, intervals between periods, reported data, areas of investigation, and researchers (Figures 4 and 5). Nolan (1927) investigated the composition of Great Salt Lake Desert (GSLD) brines. In 1925, Nolan made shallow borings across the GSLD and reported sample total dissolved solids (TDS), major ions, and groundwater levels. Nolan made major-ion measurements in the field through titration (for chloride) and by measuring the volume of precipitate formed after adding chemicals to the solution (for potassium and sulfate). Several of these sites occur on the southern edge of BSF and the area between the Silver Island Mountains and the saline pan crust (Figure 4B).

Between 1946 and 1949, 23 alluvial-fan production wells (named BW for brackish water) were drilled to depths ranging between 32 and 111 m (Bernau and others, 2023a) (Figure 1C). BW wells flowed freely (1.1 to 9.5 m³/second) when they were drilled, with reported potentiometric surfaces between 1.5 and 6 m above surface level. BW well water chemistry was reported in aggregate.

Two researchers investigated BSF chemistry between 1964 and 1972 (Figure 4C). In 1964 brine samples from shallow GSLD borings were analyzed for major ions, lithium, and TDS (Lindenburg, 1974). Between 1965 and 1967, Turk (1973) installed shallow (<9 m depth) wells across and adjoining BSF's crust, and measured groundwater levels and brine chemistry. In 1972, two brine chemistry samples from the alluvial-fan aquifer wells were collected (reported in the Water Quality Portal; Read and others, 2017).

Between 1975 and 1981 the U.S. Geological Survey performed two BSF studies (Figure 4D). Groundwater levels and chemistry were examined between 1975 and 1978 (Lines, 1978, 1979). In 1981 the U.S. Geological Survey Conservation Division measured brine chemistry from borings and wells (reported in White, 2002).

The next study period occurred leading up to the onset of the laydown in the autumn of 1997. Two groups collected measurements between 1991 and 1997 (Figure 4E). The U.S. Geological Survey measured BSF between 1991 and 1993 (Mason and others, 1995; Mason and Kipp, 1998). The Bureau of Land Management made annual measurements from a subset of wells between 1994 and 1997 (White, 2002).

Between 1998 and 2006 the Bureau of Land Management monitored brine chemistry and water levels in several wells to evaluate the laydown's impact (Figure 4F) (White, 2002). Some unpublished Bureau of Land Management measurements collected between 2003 and 2006 are compiled here (White, field notes and files including laboratory results, 1998 to 2014).

Between 2003 and 2018, Shaw Environmental, Inc. conducted biannual measurements of groundwater level and chemistry from various locations. These measurements, amounting to over 900 measurement sets, were gathered on behalf of the potash mine as part of its mine reclamation plan (Shaw Environmental, 2020). While most sites were within the potash mine, many samples were from the BSF study area. These include samples from the alluvial fan aquifer, east of the extraction ditch, and south of Interstate 80 (I-80) areas. The samples for the period spanning from 2007 to 2012 exclusively originate from this report.

Between 2015 and 2022, researchers from the University of Utah collected brine chemistry and groundwater level measurements, and between 2022 and 2023 the Utah Geological Survey collected similar measurements (Figure 4G) (Penrod, 2016; Bowen and others, 2018; Kipnis and Bowen, 2018; Lerback and others, 2019; Kipnis and others, 2020; Bernau and Bowen, 2021; Bernau and others, 2023a). The Bureau of Land Management made groundwater level and density measurements independently (White, field notes and files including laboratory results, 1998 to 2014) and in collaboration with the University of Utah in 2015.

Measurements

From May 2016 to May 2020, a precipitation sample collector with internal electrical heating was installed at the potash mine. Mine staff monitored and collected precipitation samples regularly, offering storm-event-level resolution for collected precipita-
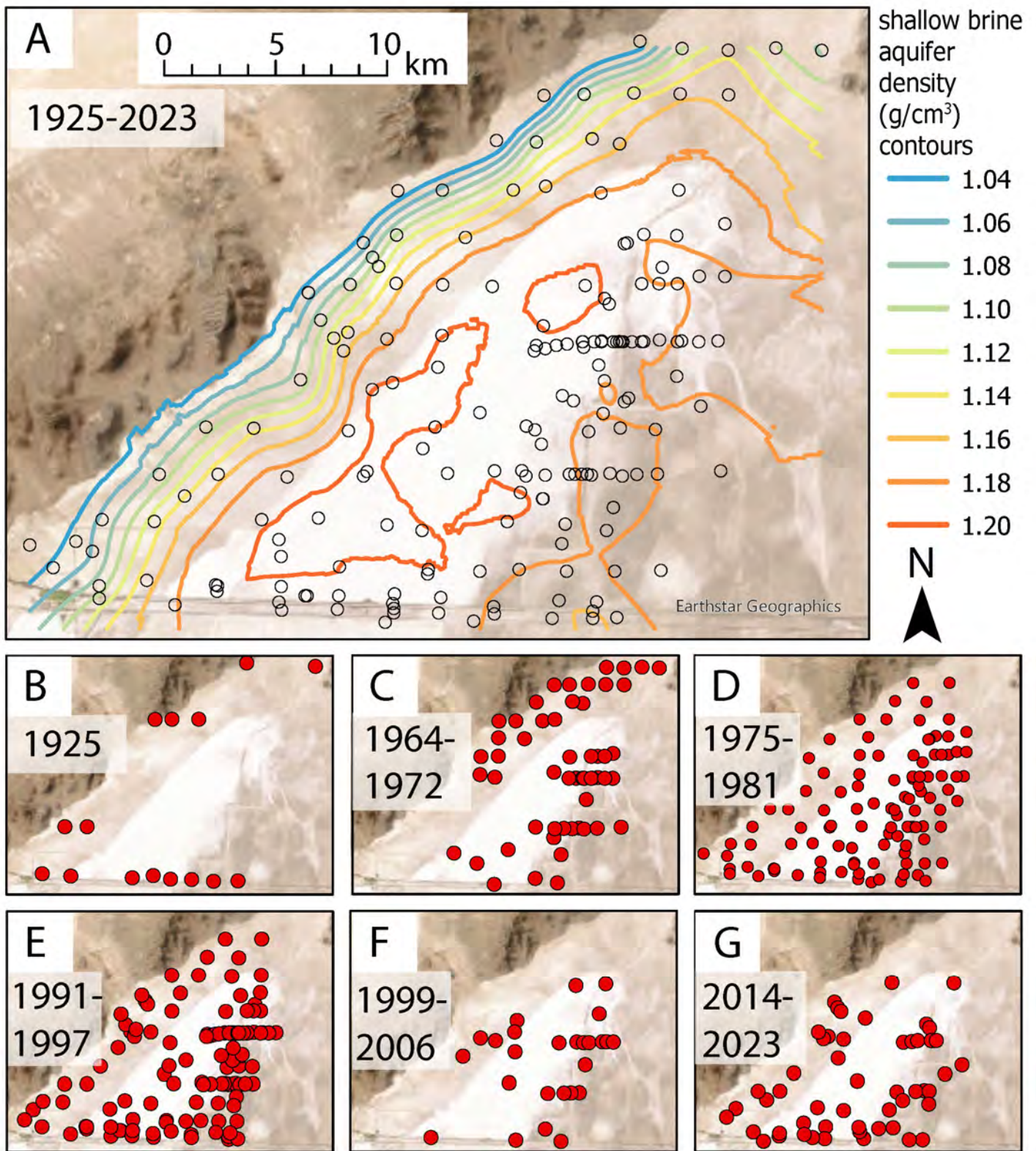
Figure 4. *Spatial distribution of shallow brine aquifer density measurements from the Bonneville Salt Flats and surrounding area. A) Compilation from density measurements between 1925 and 2023. B to G) Locations of shallow brine aquifer density measurements over time. Kriging done with Empirical Bayesian Kriging (Geostatistical Analyst) in ArcGIS.*
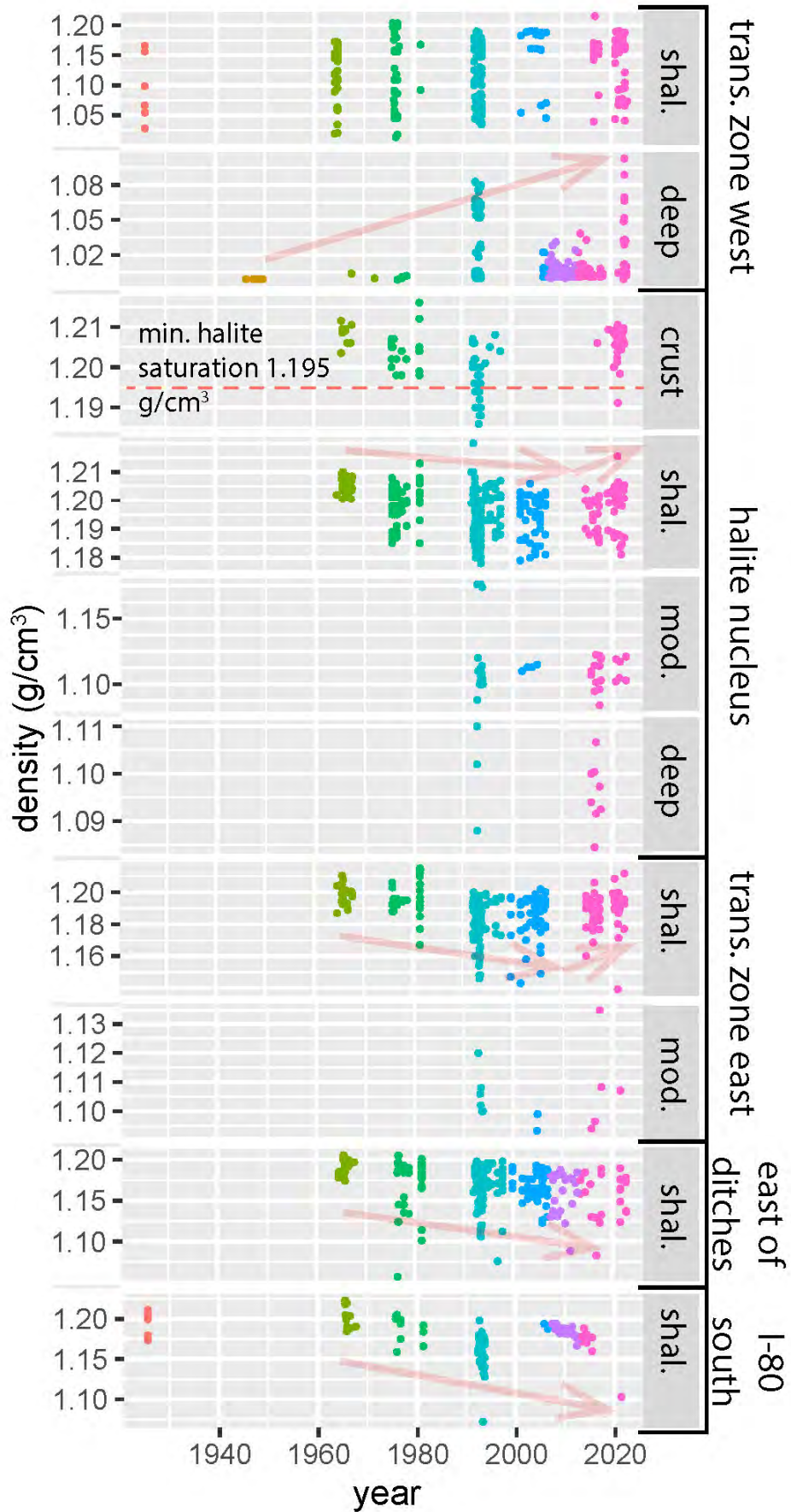
Figure 5. Brine density measurements over time (~2000 data points). Measurements are separated by area and depth of investigation. Note the difference in vertical scales. Light red arrows added to highlight trends by area.

tion. Stable water isotopes of hydrogen (δ^2H) and oxygen (δ^{18}O) were measured at the SPATIAL Lab at the University of Utah with a Picarro L2130-i cavity ring-down spectrometer. Water isotope concentrations were calibrated to laboratory standards, and values were reported as per mil (‰) relative to the V-SMOW scale.

Between 2016 and 2021, ground and surface water samples were collected in acid-washed and deionized water-rinsed bottles and returned to the University of Utah for major ion and stable isotope analyses. A subset of samples was analyzed for major ion concentrations by external laboratories using inductively coupled plasma mass spectrometry (ICP-MS/AES) and ion chromatography as reported in Kipnis and others (2020). Samples collected in 2017 and 2020 were analyzed for major ion concentrations using a portable X-ray fluorescence spectrometer (pXRF) and calibrated to the methods described in Kipnis and others (2020). Calcium concentrations and total dissolved solids were excluded from pXRF results due to data calibration challenges. Additional samples were collected in 2017 and 2018 for chemical analyses including radiocarbon (C^{14}) and tritium (^{3}H/^{3}He) dating as reported in Lerback and others (2019). Samples collected in 2021 were measured for major ions using ICP-MS and ion chromatography at the University of Utah Earth Core Facility. Samples collected in 2022 were analyzed for major ion concentrations by external laboratories (Chemtech-Ford, Utah Public Health Laboratory). Brine density values were measured in field and lab settings with a Mettler-Toledo Densito 30PX. Laboratory measurements of density at 20°C were made following the procedures of Bernau and others (2023a) at 20 °C. Before 2022, when analyzing hydrogen (δ^2H) and oxygen (δ^{18}O) stable isotopes from brine samples, solutes were removed through cryogenic vacuum extraction before stable isotope measurement. Starting in 2022, vacuum extraction was not used for brine samples analyzed for stable isotopes.

Data Quality Control

Due to the diversity in data vintages, care was taken in reviewing data quality. Because of this, changes in density were primarily focused on as density measurements are relatively robust over time and are less susceptible to methodological changes (Bernau and others, 2023a). Salinity is directly proportional to brine density and the two terms are used interchangeably here. In addition to data quality, seasonal changes in brine salinity were considered. Seasonal variations in brine density, as observed from monitoring well brines and brines extracted for potash production, indicate that samples collected during cooler and wetter winter to spring months are more likely to have depressed density measurements (Figure 6). Measurements with higher density from warmer, drier months (July to September, preferably August), are preferred for long-term evaluation. While the impact of temperature on density measurements was taken into account and corrected for whenever feasible (with a change of approximately 0.01 g/cm^3 observed between temperatures of 10 and 30 °C), it should be noted that warmer brines can dissolve more halite, resulting in higher densities (Bernau and others, 2023a). To mitigate the influence of dilution caused by flooding, it is advisable to utilize the highest recorded density at a site during a study period for long-term comparisons.

Brine chemistry reporting varied across studies. Some studies only reported field density, others reported major ion chemistry and periodically TDS, whereas others reported laboratory density measurements in addition to the measurements above. Field densities with reported temperature (if available) were corrected to the density at 20°C using Equation 11 in Bernau and others (2023a). Following the methods in Bernau and others (2023a), major ion data were used to model density using the SpecE8 module of Geochemists' Workbench® with the PHRQPITZ thermodynamic dataset (Pitzer, 1973; Harvie and others, 1980; Plummer and others, 1988; Bethke, 2013). Finally, available measurements were utilized to establish the correlation between TDS and density for BSF brines. Using the measured TDS data, a salinity for these brines was estimated. Chemical model-based estimates of density at BSF tend to underestimate density, indicating that major ion concentrations are typically underreported (Bernau and others, 2023a). When all of these measurement types and estimates of salinity were available, they were contrasted to delineate measurement quality. For long-term comparative analyses, laboratory density measurements were prioritized, then field density measurements, followed by chemically modeled density, and finally density estimated from TDS.

An additional step in data quality control was made using site-based knowledge to assess data quality and identify erroneous data to remove. For example, anomalously high density values (>1.22 g/cm^3) are not possible at BSF given its brine composition and suggest measurement errors, such as suspended sediment increasing field density measurements. An additional consideration was unusually low density measurements. For example, some samples from the years 1991 to 1993 have unusually low reported densities. Samples that contain higher levels of sodium
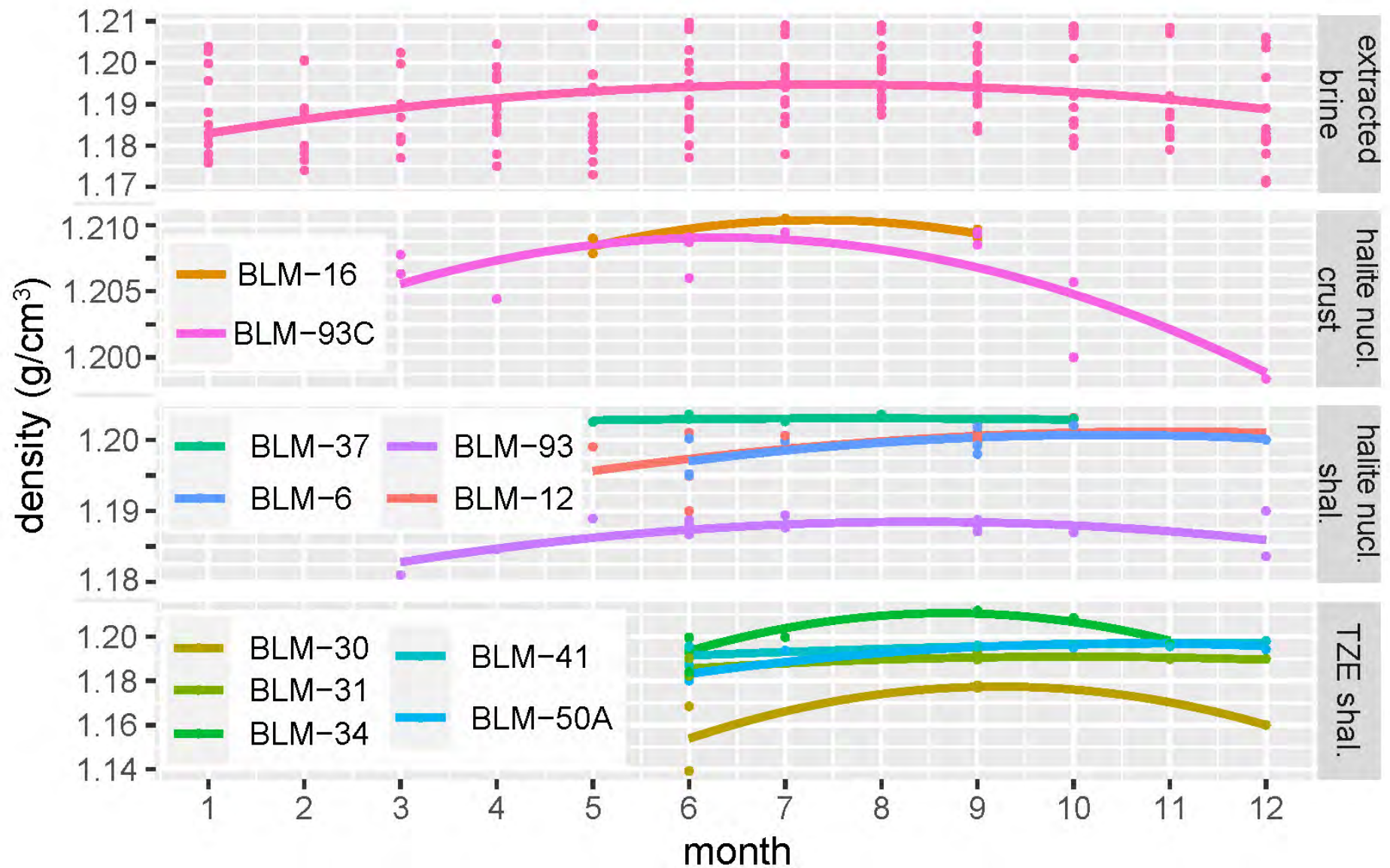
Figure 6. *Seasonality in density measurements across different sample areas. Data from 2000 to 2020 for extracted brines and 2015 to 2022 for well samples. Well locations are shown on Figure 1B. In general, brine salinity is highest and most consistent in August and September. Extracted brine density increases in the summer with peak evaporation and decreases in the winter with decreased evaporation and increased precipitation. Halite nucleus salinity reflects the impact of temperature on the solubility of halite. As the crust warms, it's brine can dissolve more halite, and increase in density. The halite nucleus shallow aquifer salinity is highest at the end of summer and lowest in the spring. Lower salinity in early spring may reflect the upward movement of deeper, less saline brine as the surface warms (Bernau and Bowen, 2021). Brine densities in the transitional zone east shallow aquifer generally peak in September, potentially reflecting evapoconcentration.*

and chloride ions exhibit greater densities. When these samples reach halite saturation, as they are when they are in contact with halite for a sustained period, any changes in density are limited by the process of halite dissolution or crystallization. In the case of brines in contact with halite, there have been instances where the reported densities were below the density of halite saturation. This was exceptionally clear in samples from the crust-hosted aquifer with reported densities below 1.18 g/cm^3, which is below halite saturation (1.195 g/cm^3 minimum at halite saturation at BSF) (Figure 5). These anomalously high and low measurements were omitted from analyses. The final step in data quality control used known spatial distributions of salinity to identify unusually high or low density measurements, which were then assessed and removed or kept if they were consistent with additional site measurements during that period.

Individual Well-Based Analysis

Given the spatial heterogeneity of the brine chemistry, it is important to evaluate this system at specific sites over time in addition to characterizing the overall system. Well sites were selected for individual well-based analysis if they had multiple measurements across several study periods (a site could include past borings and wells of similar depths at the same location). The Kendall test and linear regression (Kendall package and linear model function in the R© coding language) (Wilkinson and Rogers, 1973a; Hipel and McLeod, 1994; R Core Team, 2021; McLeod, 2022) were applied to site data to identify locations with statistically significant (p-value <0.05) long-term trends in density change. The Kendall test assumes that long-term trends are consistent and have not changed. Because measurements were not uniformly distributed over time they could not be used for Mann-Kendall or break-point analyses.

Areas of Investigation

To better describe changes and aggregate data, studied areas were divided spatially and by aquifer depth (Figure 1B and D).

Lateral Divisions

Areas of investigation were divided based on surface mineralogy, potential groundwater flows, fabricated structures (the interstate highway and drainage ditches), and lateral salinity (density) gradients (Figures 1B and 4A). Similar terminology based on hydrological fluxes and sedimentology has been used to establish lateral divisions in other saline pans (Munk and others, 2021). From west to east, these areas are the transition zone west (TZW), halite nucleus, transition zone east (TZE), east of ditches, and I-80 south (Figure 1).

The TZW area includes the region to the west of the persistent halite crust up to the Silver Island Mountain front. This area consists of a mudflat (inner TZW) which transitions into a higher-elevation mudflat with dunes and intermittent vegetation (outer TZW). The location of the inner and outer TZW is reflected in USDA soil maps, where the inner TZW area corresponds with a playa unit and the outer TZW area corresponds with a playa-saltair complex with 0 to 1% slope (Soil Survey Staff, accessed March 2023).

TZW waters flowed toward the saline pan in the past. Before 1946, at least two now-dormant springs near the mountain front flowed between 0.02 and 3.4 m^3/minute (Utah Division of Water Rights database). Lines (1979) reported a decline in hydraulic gradient between the alluvial fan and the saline pan. Mason and Kipp (1998) also reported outer TZW desiccation fractures (some >1 m wide) and no hydraulic gradient between the saline pan and TZW. Kipnis and Bowen (2018) also noted a decline in alluvial-fan aquifer groundwater levels beyond historical norms after 1998.

The halite nucleus consists of an area with a persistent halite crust (up to 1.5 m thick). The minimum halite extent, as mapped across several decades of aerial imagery, was interpreted as the halite nucleus' boundary. The salt crust aquifer only occurs beneath the halite nucleus. Nolan (1927) noted the halite nucleus extended south to the area of the current potash mine in 1925.

The TZE is between the halite nucleus and the eastern brine extraction ditches. This area is covered by ephemeral halite crust (precipitated from standing water) and efflorescent salts (primarily halite) overlying authigenic gypsum sand (Bernau and Bowen, 2021). The area to the east of the brine collection ditches is hydraulically connected to the greater GSLD. The east of ditches area is defined as the region that is closest to the drainage ditches and is likely to be impacted by brine extraction. The final area of investigation is the zone immediately to the south of I-80 that is impacted by brine extraction ditches and is isolated from the saline pan by I-80, which prevents overland flow and limits subsurface brine movement (Mason and Kipp, 1998). Before manmade structures were built at BSF, brines could flow from the southern and eastern parts of the GSLD to BSF. Evidence of this can be seen today in aerial and satellite imagery of seasonal ponds that develop to the

southeast of the potash mine (Radwin and Bowen, 2021).

Aquifer Divisions

Previous studies characterized basin-fill, alluvial-fan, and shallow brine aquifers by water chemistry and recharge rates (Turk, 1973; Lines, 1979; Mason and Kipp, 1998). Aquifers and samples are delineated by depth (Figure 1D); these include surficial samples, such as brine collected from extraction ditches and the laydown, and subsurface samples, which are the focus of this study. Depth intervals are described from shallowest to deepest. The crust-hosted wells occur in the halite nucleus, where they are screened within 1 m of the surface. Brine samples from this aquifer should be at halite saturation because the aquifer is hosted in halite. The shallow aquifer occurs directly under the crust-hosted aquifer in the halite nucleus and is in contact with the surface elsewhere. The shallow, moderate, and deep aquifers occur within lacustrine to saline sediments which consist of carbonate-rich mud and gypsum (with gypsum only occurring in deep basinal muds, >50 m depth) (Shuey, 1971; Stephens, 1974; Oviatt and others, 2020; Utah Division of Water Rights database).

The shallow basinal mud aquifer (reported as the shallow brine aquifer in other publications) occurs from ≥0 to <10 m depth. This aquifer ranges in salinity from 1.04 to 1.21 g/cm^3 (Figure 4A), is fractured, and contains brine-shrimp fecal pellet intervals, contributing to a higher hydraulic conductivity than anticipated from its mean grain size of silty clay (Turk and others, 1973; Lines, 1979). The aquifer's fractures occur in hexagonal patterns. Turk and others (1973) proposed that the fractures formed through osmotic desiccation or synaeresis. Where multiple wells exist in the same aquifer depth range at the same site, the shallower well or the well with a longer reporting span was used for multi-decadal single-well analyses. Turk (1973), Turk and others (1973), and Lines (1979) estimated the total thickness of this aquifer to be between 4.5 and 8 m. The largest source of recharge to the shallow brine aquifer is meteoric water infiltration through the surface (Mason and Kipp, 1998). Major aquifer discharge sources are the pumping of ditches along the eastern margin of the saline pan and subsurface flow south underneath I-80 (Mason and Kipp, 1998).

Wells screened in the moderate depth aquifer occur within ~10 to 30 m depth and only occur within the halite nucleus and TZE. Permeability in the moderate depth aquifer is far lower than the shallow aquifer (Mason and Kipp, 1998), possibly due to the absence of fractures and limited connection with overlying higher-permeability aquifers. Alluvial-fan brackick water (BW) aquifer wells (>10 to 150 m depth; measured wells occur between 22 and 111 m depth) are screened in muds (which occur from surface to 8 to ~70 m depth across BW wells) to alluvial-fan gravels (Stephens, 1974; Bernau and others, 2023b). The observation well (OW) alluvial-fan aquifer wells (Figure 1C) do not have any reported logs with them, but the OW wells closer to the Silver Island Mountain front reach depths known to intersect gravel lenses.

Two wells at BSF's center occur within deep (~30 to ~250 m depth) basinal muds and possibly bedded gypsum; this lithology interpretation is based on deep brine well logs from the potash mine to the south (Utah Division of Water Rights database; Bernau and others, 2023b). These deep basinal wells have 3-m-long screens at ~70 and 150 m depth. Underlying deep basinal muds are basinal gravels, which occur at depths of >250 m. The potash mine uses wells in basinal gravels as a source of potassium-rich brine. The basinal gravel aquifer consists of gravels, conglomerates, and Tertiary volcanic rocks (Stephens, 1974). Water rights reports and data reported in the potash mine reclamation plan (Shaw Environmental, 2020) of basinal gravel wells show the deep brine aquifer's potentiometric surface declined ~20 to 30 m between the 1950s and 2010s.

RESULTS

Here, chemical results are analyzed in a spatial and temporal context, progressing from west to east, covering the period from 1925 to 2023. Datasets with insufficient information to differentiate trends are not discussed. For example, most trace elements had insufficient data to identify spatial or temporal changes.

Transitional Zone West

Compositionally, many TZW samples differ markedly from other BSF samples (Figure 7). They have higher relative proportions of sulfate (SO_4^{2-}), alkalinity (as HCO_3^-), calcium (Ca^{2+}), and magnesium (Mg^{2+}) than other areas because they have lower concentrations of sodium (Na^+) and chloride (Cl^-) (especially in the alluvial-fan aquifer wells). Shallow aquifer TZW brines show a clear decrease in magnesium between the 1964–1972 and 1999–2006 periods, with increasing magnesium after the 1999–2006 period (Figure S1). Additionally, lithium (Li^+) concentrations are much lower in the TZW than in other areas (Figure S2).
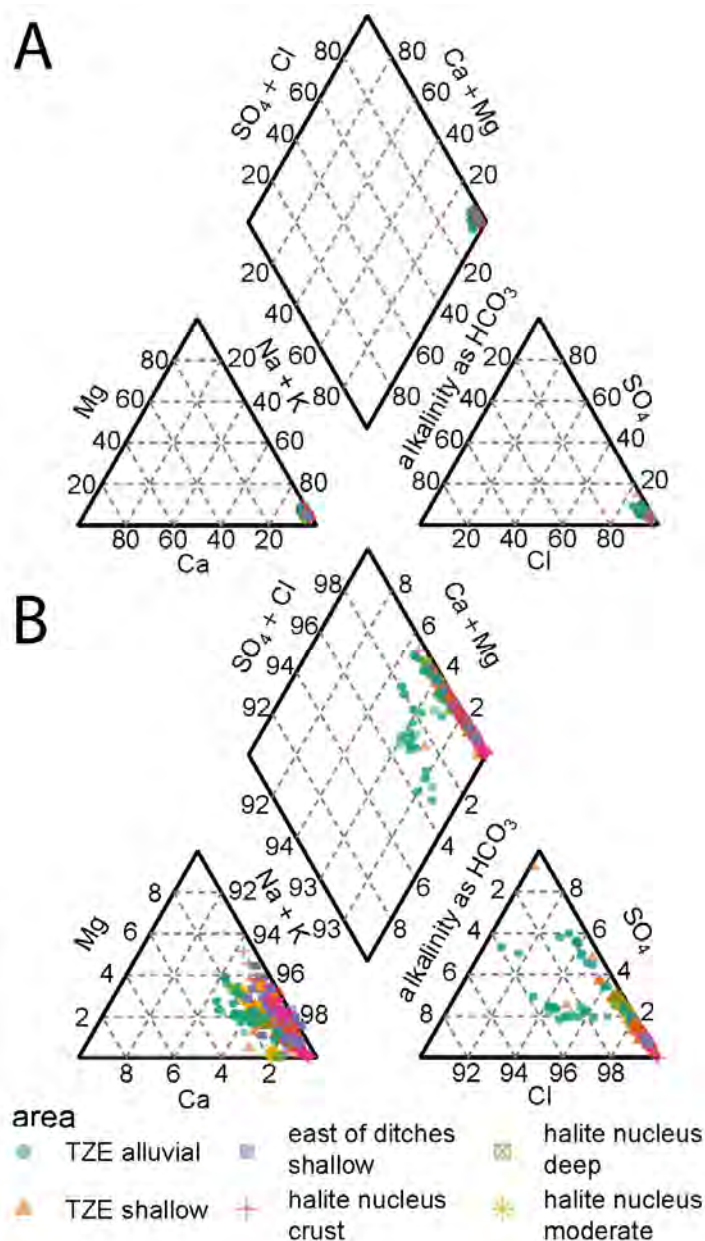
Analysis of individual wells in the TZE shallow

Figure 7. Piper diagram of geochemistry measurements across BSF at A) normal scale, B) magnified scale. A) The high salinity system dominated by Na and Cl makes differentiating between sites based on relative ionic content challenging. B) Differentiation between sites when examined at the 90/10/10 percentile values.

aquifer identified two areas of increasing salinity (Figures 8A and B). The first segment occurs near the OW transect (Figure 1C). The second segment occurs mid-way along the saline pan, where the inner TZW is wider because of a low-lying Silver Island Mountains pass connecting this area to Pilot Valley.

Aggregate analysis of the TZW shallow aquifer (Figure 9A) indicates that the outer TZW area has experienced an increase in salinity over time. In contrast, the inner TZW area does not exhibit consistent changes in salinity. The inner TZW aggregate results contrast with those of the individual well analyses,

possibly from differences in sampling location across studies. Over time, the outer TZW area has had marked declines in groundwater levels; several shallow aquifer wells were persistently dry during the 2013–2023 study period.

Stable water isotope measurements from the TZW shallow aquifer indicate that it is isotopically lighter (meaning it originates from less evaporated waters or precipitation from cooler periods) relative to other shallow aquifer areas (Figures 10 and 11). Similar to the shallow aquifer in other areas, a negative shift in TZW shallow aquifer deuterium excess values (Dansgaard, 1964) suggests a change to more evaporated waters over time (Figure 11).

The alluvial-fan aquifer has had notable declines in groundwater levels since the early 1990s (Figure 3E) (Kipnis and Bowen, 2018). In addition to hydraulic head changes, between 1993 and 2022 there have been marked changes in brine density and δ^2H and $\delta^{18}O$ values. Furthermore, the spatial distribution of these values over time (Figures 12–15) reflects changing groundwater sourcing from mountain front sourced waters to more evaporated waters from the saline pan area.

The BW production well transect shows increasing density and a shift to heavier δ^2H and $\delta^{18}O$ isotopes over time (Figure 12). The largest density increase is concentrated at the center of the active production field (where produced waters now exceed a density of 1.05 g/cm³), with smaller density increases occurring on the edge of the active field (wells at 1.8 and 4.2 km). There are some exceptions to the correlation between increased density and generally heavier water isotopes. Waters from a well at 4.2 km had relatively low densities, but heavier isotopic values. This indicates that some waters originate from precipitation under warmer conditions or from evaporated waters (as suggested by water isotopes) that do not have an elevated salinity.

Observations from the OW well transect, which spans the inner to outer parts of the alluvial-fan aquifer (Figure 1C), inform the interpretation of observed changes in BW chemistry (Figures 13 to 15). Figure 13A to C, a cross section of OW measurements over time shows an increased density gradient towards the basinward direction (to the east) with a transition in salinity between 1 and 2 km. Similarly, Figures 15A and D show a transitional zone between the alluvial-fan and basinal δ^2H and $\delta^{18}O$ values in the year 1993 occured between 1 and 2 km along the transect. The δ^2H, $\delta^{18}O$, and deuterium excess values observed in mountain front-adjacent alluvial-fan samples suggest these waters are sourced from winter precipitation that has undergone minimal evaporation and fractionation (Figure 11). The deuterium excess values of all
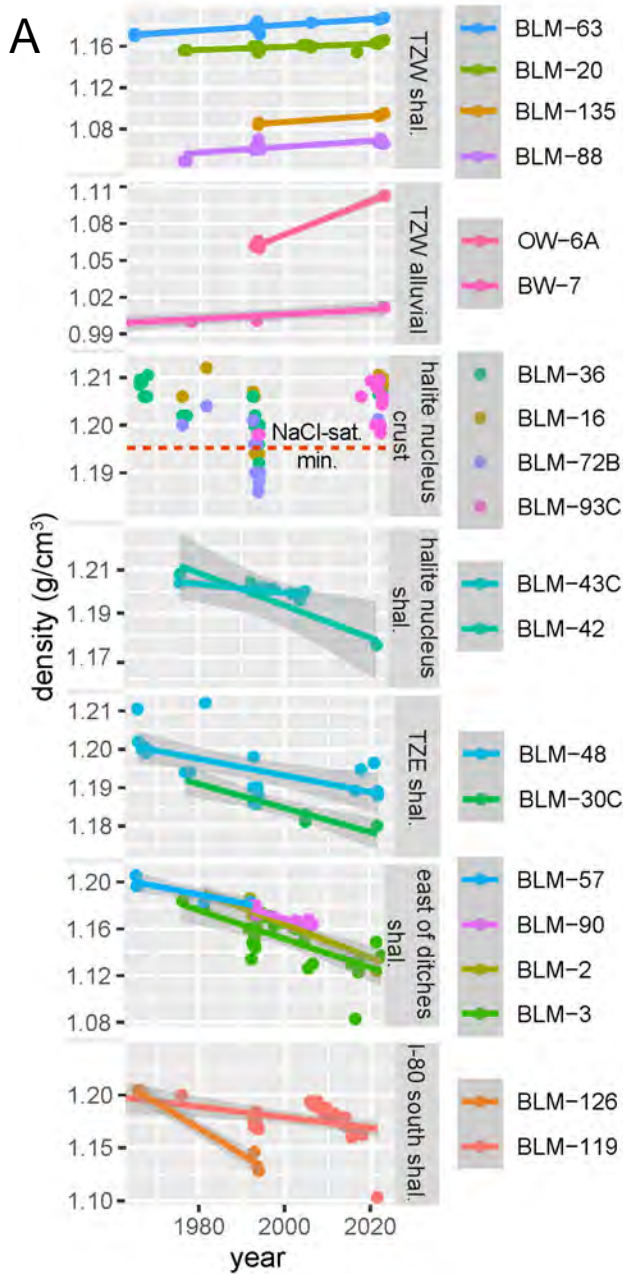
Figure 8. A). Select well trends in density through time. Samples from east of ditches, TZE, and I-80 south areas are all from wells screened in the shallow aquifer. See Figure 1B well locations. B) Sites from Fig. 8A with a statistically significant change in salinity. Color is used to denote change in density. Size denotes the relative fit of change with time (higher r² shows a stronger correlation of change with time). All wells in B) are in the shallow aquifer except for the alluvial-fan aquifer well in the southwest corner of the map.
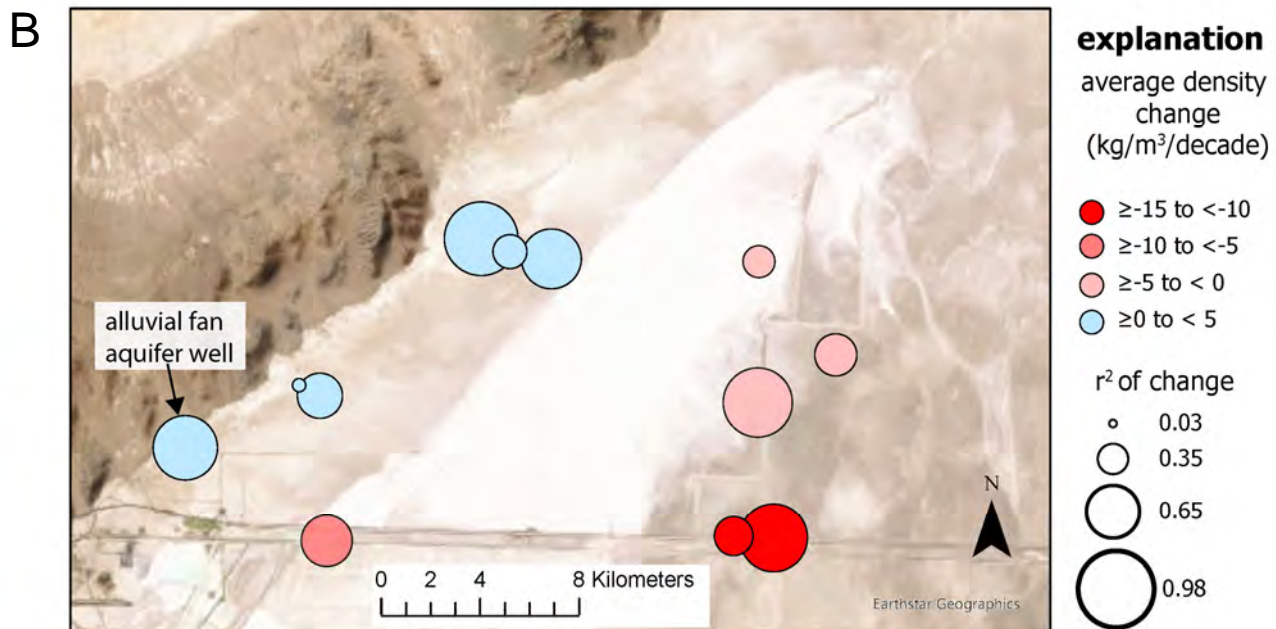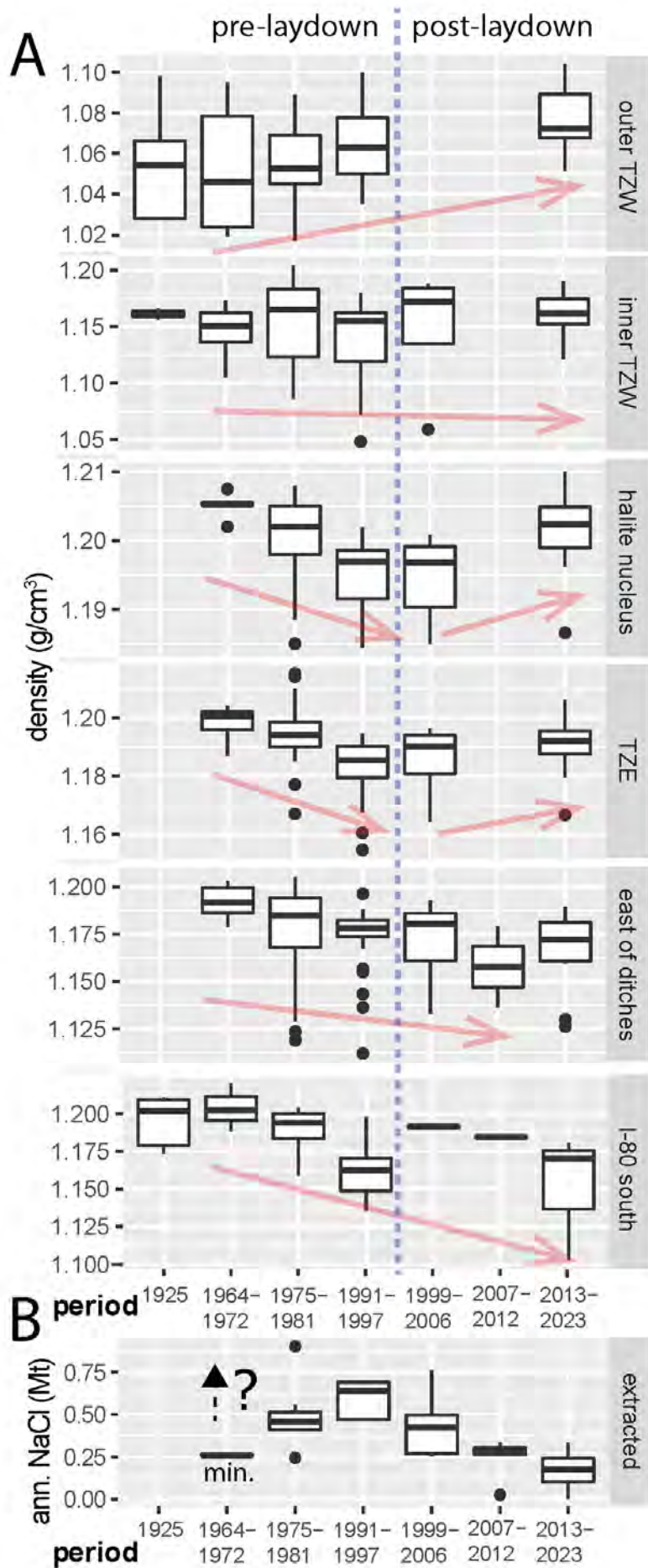
Figure 9. Box and whisker plots of changes in (A) shallow aquifer brine density across different areas over time and in (B) brine extraction rates over time. Individual well data has been averaged for each sampling period to minimize the effect of sampling bias on results. Note that sampling has not been consistent at the same wells over time, making trends identified here different from those identified in Figure 8A. Extraction rates before 1991 are primarily estimated and have a high range of uncertainty.
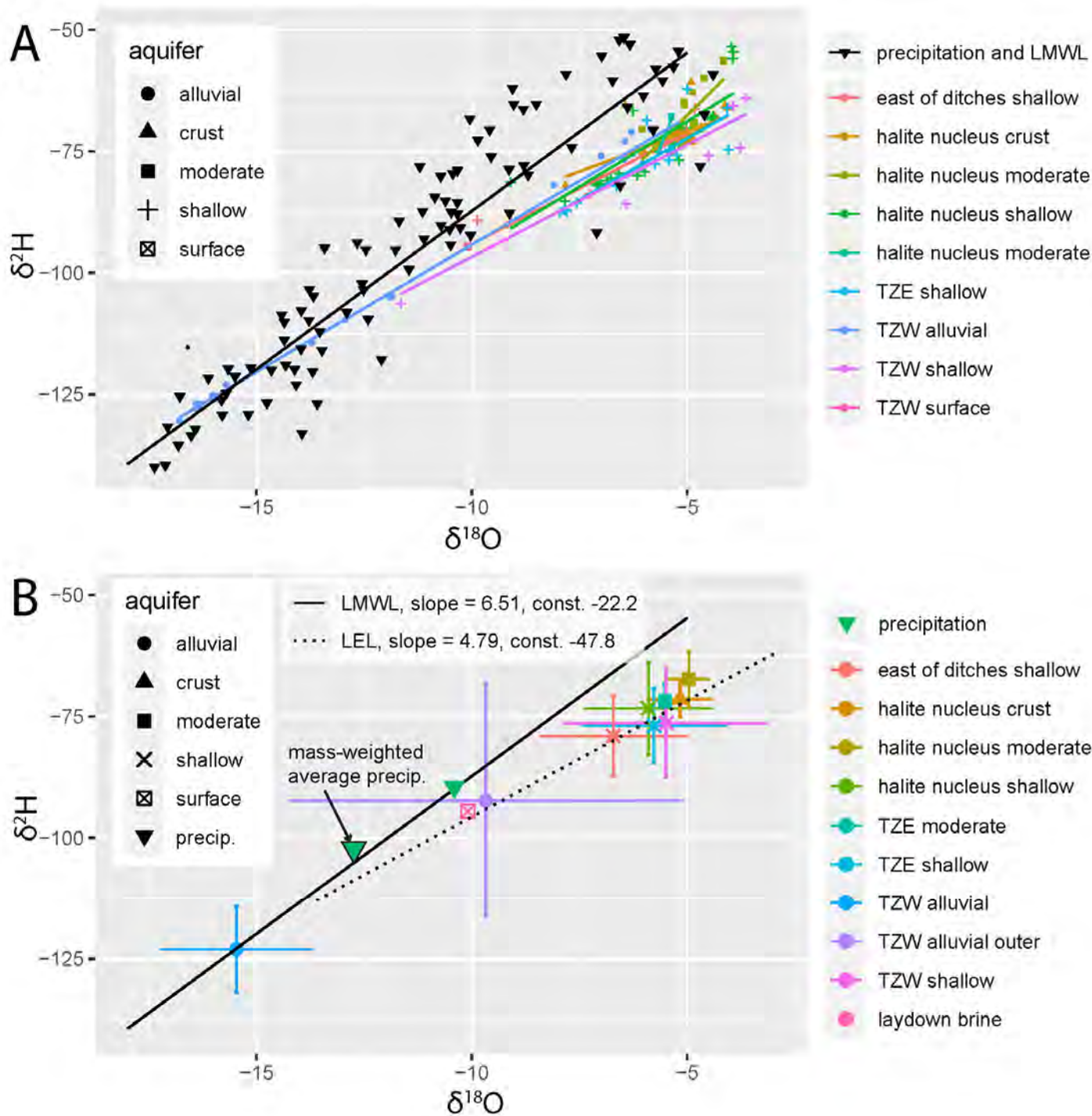
Figure 10. *Spatial changes in water δ^2H and $\delta^{18}O$. A) All isotope data. B) Average isotope values by area with standard deviation in error bars. TZE alluvial outer wells indicate OW wells located >1 km east of transect start. LMWL is the local meteoric water line. LEL is the local evaporation line.*

other areas suggest their composition was influenced by evaporation. Nevertheless, the absence of a proportional increase in deuterium excess values with increasing brine density implies that the salinity of the brine arises not only from evapoconcentration but also from the dissolution of salt (Figure 11D). These data strongly support the theory that high salinity in the halite nucleus is maintained by salt crust dissolution.

Between 1993 and 2022, the hydraulic gradient shifted to mountain front-directed flow with a 10 m change in the hydraulic head at 0 km in the OW transect (Figure 14A to F). Hydraulic head was corrected for density to assess the effect of density on groundwater flow by using Equation 1 (Figure 14D and E) (Post and others, 2007).

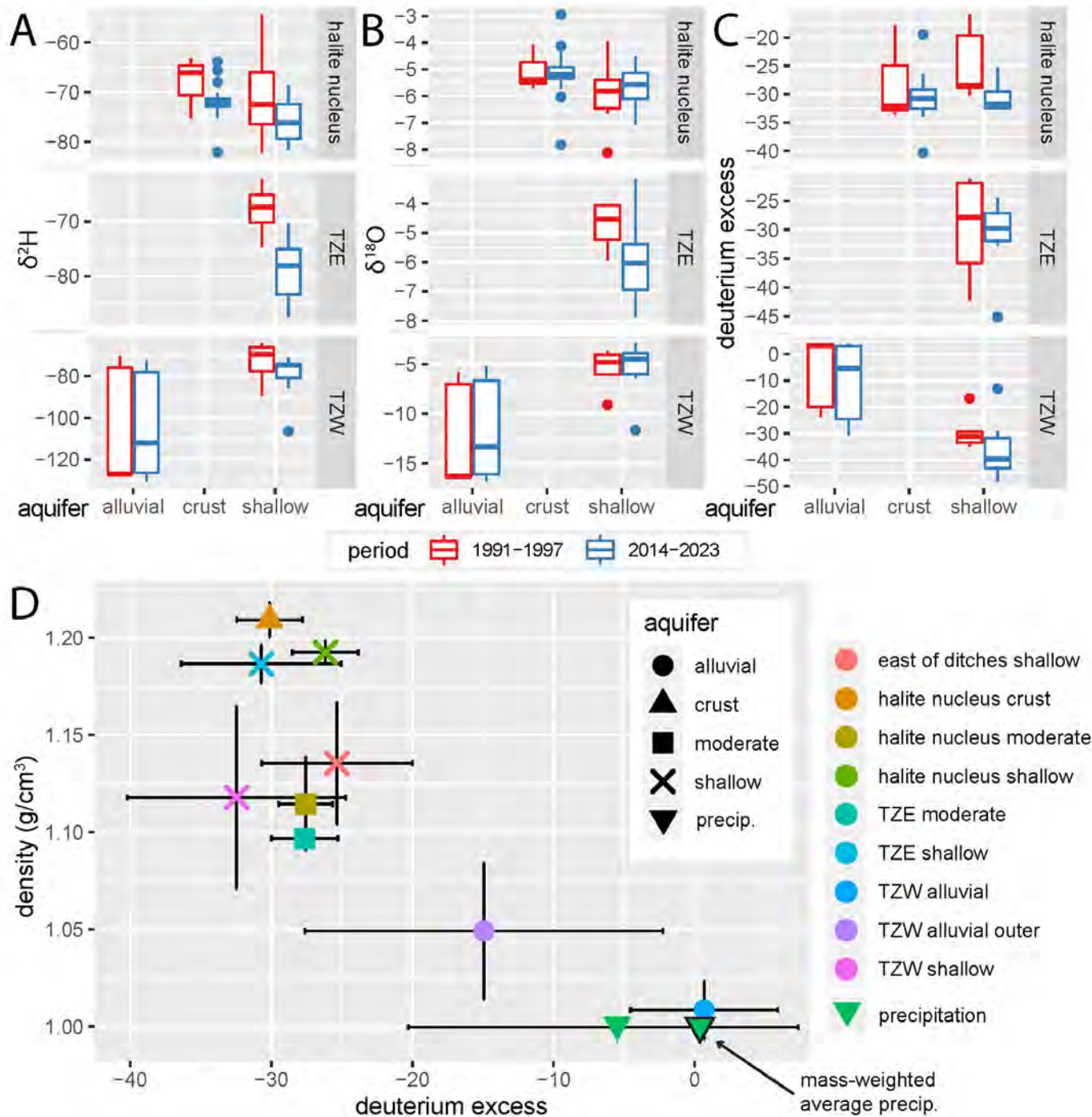$$h_1 = \frac{\rho_2}{\rho_1} h_2 - \frac{\rho_2 - \rho_1}{\rho_1} z \qquad \text{(Equation 1)}$$

Figure 11. *Comparison of stable isotopes by area and aquifer over time. A) δ^2H, B) $\delta^{18}O$, C) deuterium excess, and D) deuterium excess relative to density.*

where ρ_1 is the reference density to adjust the sample to (freshwater density, 1.0 g/cm³); ρ_2 is the density of the well-water (calculated from the average density of water's produced from a well in a period); h_2 is the height of the water level above a datum (mean sea level); z is the elevation (above the sea-level datum) of the mid-point of the well's screened interval; and h_1 is the equivalent head relative to the datum.

Between the years 1993 and 2022, there was an approximately 12-meter change in hydraulic head at the center of the BW production field. Interestingly, the basal head level observed in the OW wells (Figure

14b) for 2022 closely matches the head observed at the center of the production field in Figure 3E. This similarity in head change, despite a lateral offset of over 4 kilometers, indicates a high level of hydraulic connectivity across the BW alluvial-fan aquifer wells.

Correcting for the effect of density on hydraulic head has a significant impact on inferred water flow, as shown in Figure 14. In 1993, it becomes evident that groundwater primarily flows towards the west when the density correction is applied. Without this correction, groundwater flow would have been interpreted as moving towards an elevation of approxi-
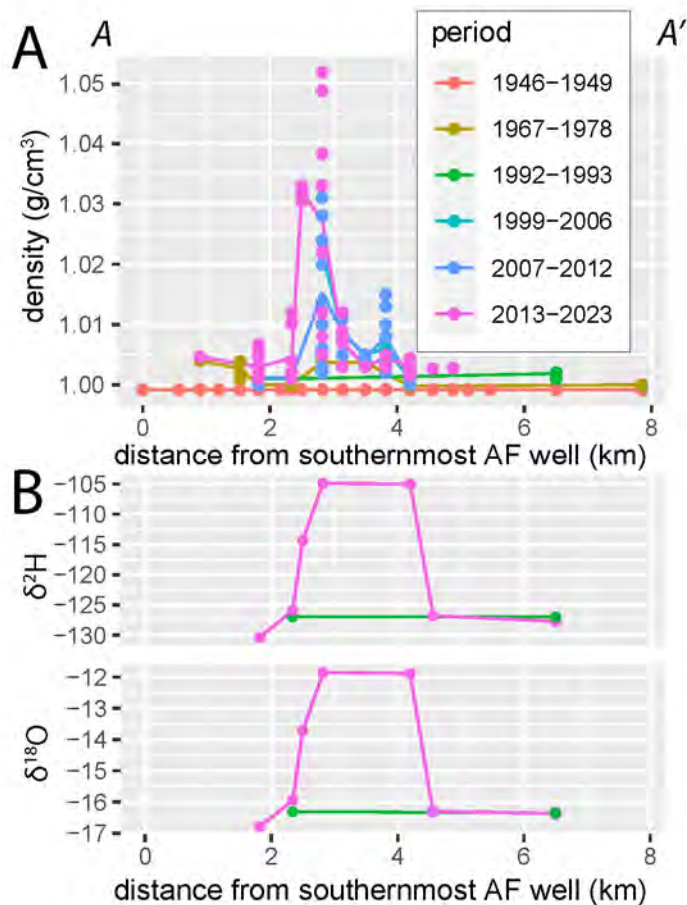
Figure 12. BW well cross section with salinity and water stable isotopes over time. Location of A to A' is shown on Figure 1C.

mately 1240 meters above sea level at 2 kilometers along the transect. In 2022, the density correction has a relatively smaller impact, but it still highlights that groundwater primarily flows in a westward direction, and downward vertical flow is less significant than what the uncorrected head measurement would suggest.

Changes in OW-brine density indicate that brine transports salt mass from the halite nucleus crust and underlying aquifers and towards the alluvial fan. Changes are concentrated on the basinward side of the OW cross section; where salinity has increased by 0.04 g/cm^3 at 2.6 km at ~1255 meters above sea level and by ~0.01 g/cm^3 at ~1215 meters above sea level. The cross-sectional view of salinity change (Figure 13C) shows a saline "nose" with brine migrating down and then west and upwards towards the alluvial fan (possibly along gravel lenses).

OW-transect wells have the largest stable-isotope changes of any area in the dataset. The largest change occurs at ~0.8 km at ~1245 meters above sea level (Figure 15C and F). This change reflects the movement of basinal water in the direction of the mountain front and is also shown in the 2022 cross-sectional view of isotope data (Figure 15B and E), which

shows a blurring of the delineation between alluvial- and basinal-sourced water that was evident in the past (Figure 15A and D). These OW changes suggest that the BW well at 4.2 km has tapped basinal waters but has not yet sourced waters from areas with elevated salinity.

Halite Nucleus

Figure 5 illustrates declining halite nucleus brine density with depth. Crust aquifer brine is halite saturated (>1.195 g/cm^3); the shallow aquifer has high salinity (1.175 to >1.195 g/cm^3), and the moderate and deep aquifers have lower salinities (1.09 to 1.175 g/cm^3 and 1.08 to 1.11 g/cm^3, respectively). Mason and others (1995) showed this decline in salinity with depth by measuring pore water chemistry at multiple depths.

Individual well plots show no change in density over time in the halite nucleus crust samples (Figure 5). Past research suggested that the crust aquifer potassium concentrations decreased between the 1960s and the 1970s (Lines, 1979); subsequent analyses, however, show no long-term change in potassium from the 1960s baseline (Mason and Kipp, 1998; White, 2002) (Figure S3). Calcium concentrations decreased between the 1960s (from a high of ~1700 mg/L) to an observed low in the 1991–1997 period (~1100 mg/L) and then increased (Figure S4).

There is a notable isotopic lightening in the halite nucleus crust aquifer for δ^2H values between the periods of 1991–1997 and 2013–2023. Shallow aquifer samples show a similar change in δ^2H. This trend is not seen in the δ^{18}O values, which slightly increased in both aquifers.

Two wells showed decreasing halite nucleus shallow aquifer salinity over time (Figure 8). Aggregate data show a long-term density decrease with brines becoming halite undersaturated between 1964 and 1997 (Figure 9A). Afterward, density remained stable and then increased during the 2013–2023 period. Spatial differences in sampling location over time may influence this trend. In contrast to density measurements, the halite nucleus shallow aquifer sodium and chloride concentrations appear to consistently decrease over time (from 105 to 90 g/L and from 180 to 150 mg/L, respectively) (Figures S5 and S6), highlighting the problematic nature of accurately measuring high-salinity brines (Bernau and others, 2023a). Calcium concentrations are positively correlated to changes in density over time in the halite nucleus shallow aquifer while sulfate concentrations are negatively correlated to density changes (Figures 9, S4, and S7).

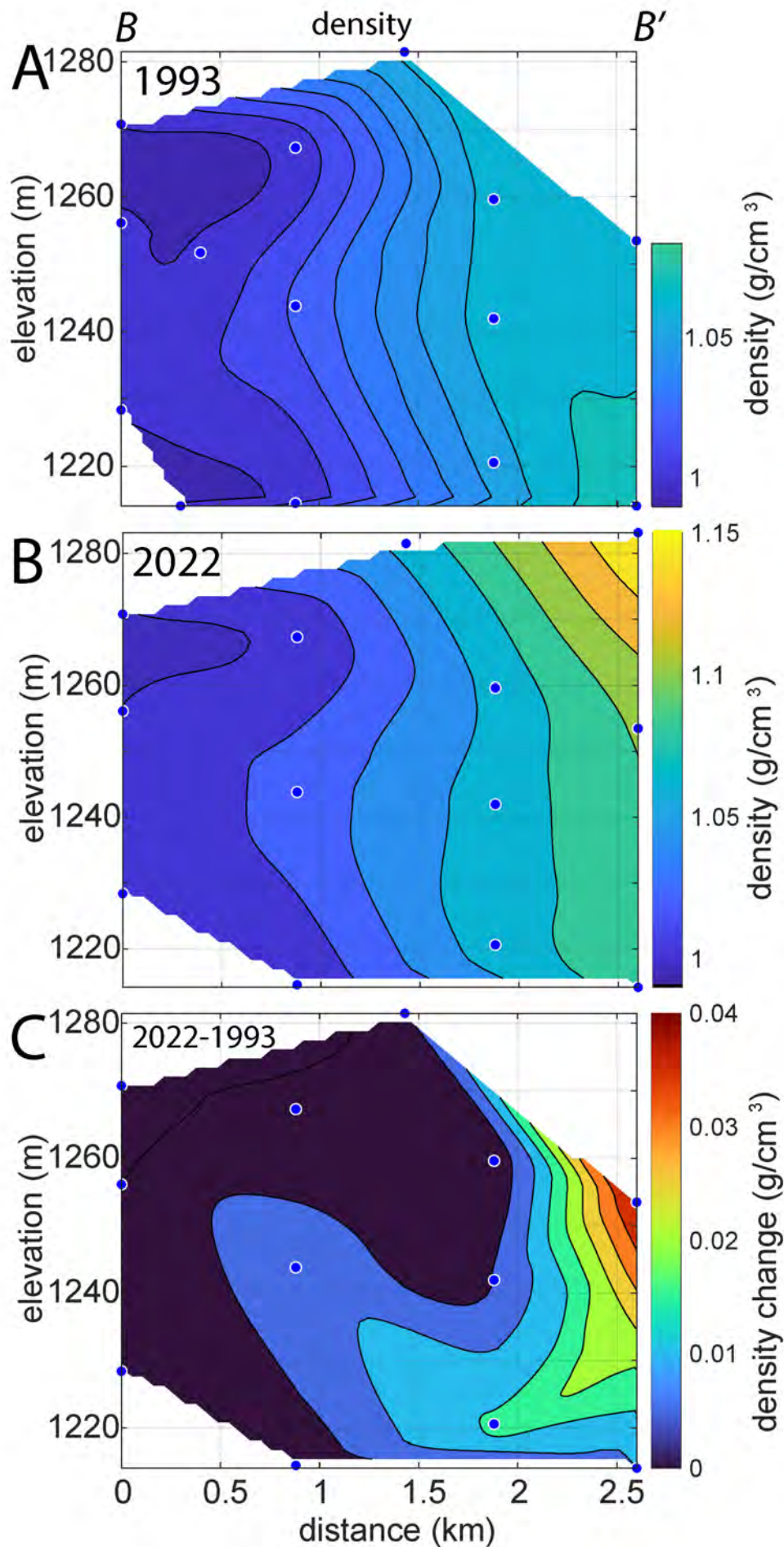Moderate and deep halite nucleus aquifer wells

Figure 13. OW cross section density. Density in (A) 1993, (B) 2022, and (C) change in density between 1993 and 2022. Each blue dot represents the midpoint of a well's screened interval. The location of B to B' is shown in Figure 1C. (~40x vertical exaggeration). Elevation is meters above sea level. Local surface elevation (not shown) is 1284.9 to 1293.0 m. Note that A & B use the same color scales with only the applicable range for each segment being shown.
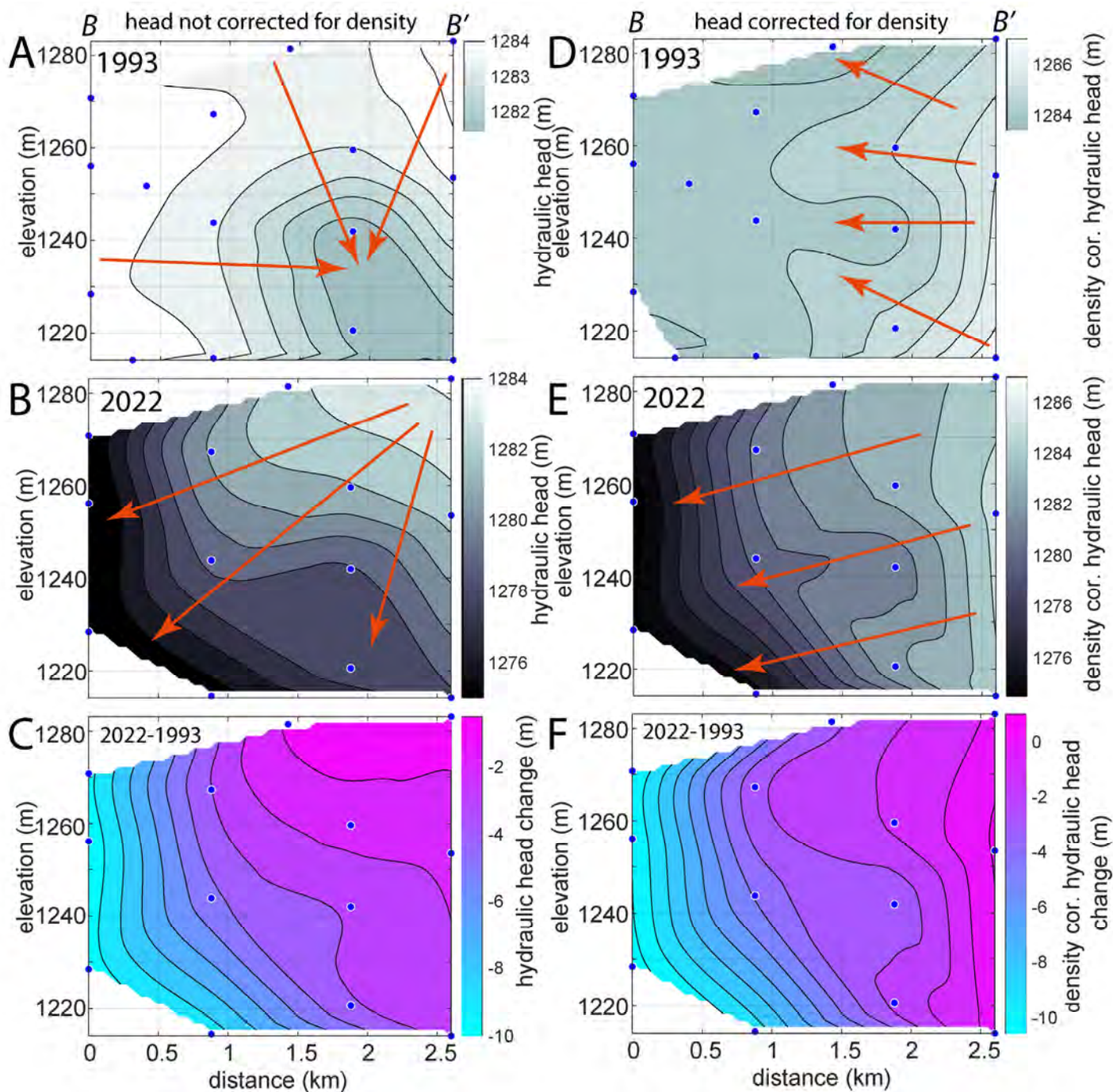
Figure 14. *OW cross section of hydraulic head over time. (A to C) Measured hydraulic head measurements and (D to F) hydraulic head measurements corrected for density. Note the impact of density correction on apparent flow direction (red arrows). Note that A & B, and D & E use the same color scales, respectively, with only the applicable range for each segment being shown. Each blue dot represents the midpoint of a well's screened interval. The location of B to B' is shown in Figure 1C. (~40x vertical exaggeration). Local surface elevation (not shown) is 1284.9 to 1293.0 m. Elevation is meters above sea level.*

have a limited sampling history over a small spatial extent, and no unequivocal changes in their composition were observed. The moderate depth aquifer had the highest observed sulfate concentrations of any area and aquifer (Figure S7).

Transitional Zone East

Two wells showed clear decreases in TZE shal-

low aquifer salinity over time (Figure 8). Aggregate TZE shallow aquifer measurements show salinity decreased through the 1991–1997 period and increased afterward. In contrast to density (and similar to the halite nucleus shallow aquifer), reported sodium and chloride concentrations have decreased over time. Magnesium concentrations at TZE reflect observed density changes. Similarly, TZE shallow aquifer potassium concentrations decreased up to the 1991–
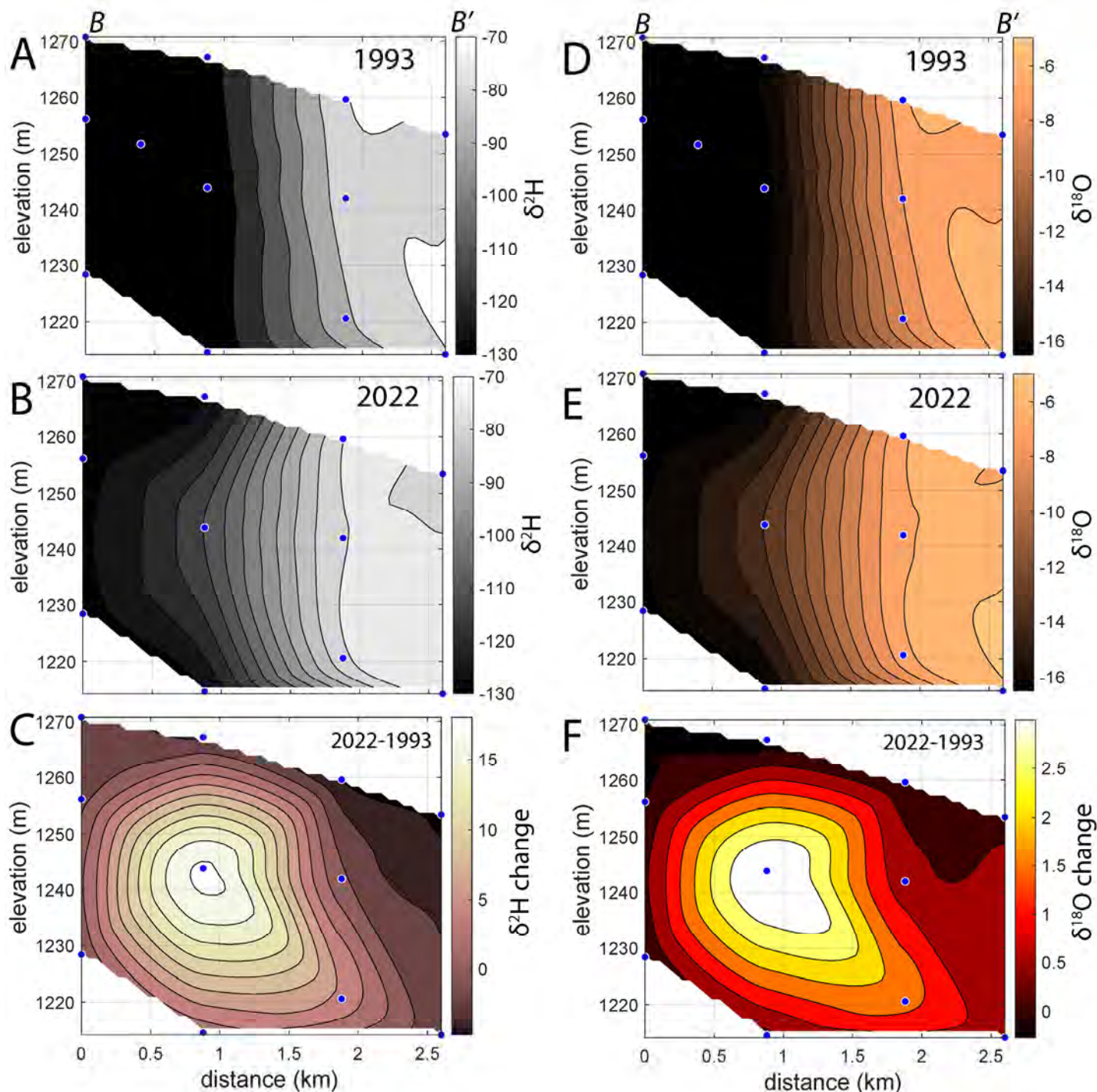
Figure 15. *OW cross section of water stable isotopes (δ²H: A to C, and δ¹⁸O: D to F) over time. A & B and D & E use the same color scales, respectively, with only the applicable range for each segment being shown. Each blue dot represents the midpoint of a well's screened interval. The location of B to B' is shown in Figure 1C. Note the vertical scale differs from Figures 13 and 14. (~40x vertical exaggeration). Local surface elevation (not shown) is 1284.9 to 1293.0 m. Elevation is meters above sea level.*

1997 period; there were no changes in the following period. Measured δ^2H became lighter between the 1991–1997 and 2013–2023 periods (Figure 11A).

Extracted Brines

Here, changes in brine extracted from the eastern collection ditches are described. NaCl removal from subsurface flow to the south (Mason and Kipp, 1998) is not considered in these values. Sustained brine production at BSF began in 1939 (Bingham, 1980); since then, the location and volume of brine extraction for potash production at BSF have varied over time (Figure 9B). Before 1966, the Salduro Loop ditch at the center of BSF (Figure 1B) was used to harvest brine; this ditch was likely constructed after sustained production began in 1939, and it is present in 1946

aerial imagery. Hadzeriga (1964) reports an initial 1% KCl and 21% NaCl weight content of brines used for potash production. The mass of potassium produced annually from the shallow aquifer since 1968 is reported in the potash mine's estimated resources and reserves report (Agapito, 2022). Production from BSF area and the area south of I-80 was lumped together, as such these values can only be used to provide an estimate of brine extraction from BSF over time. The eastern ditches at BSF have been pumped intermittently since 1963 (Lines, 1979). An estimated 0.26 Mt NaCl/year was extracted from the eastern ditches between 1966 and 1972 (Stephens, 1974) (Figure 9B). Lines (1979) reports extraction of >0.25 Mt NaCl/year in 1976. Mason and Kipp (1998) estimated 0.47 Mt NaCl/year extraction. White (2004) reports that brine extraction between 1995 and 1998 was between 0.45 and 0.94 Mt NaCl/year. Brine extraction rates between 2001 and 2021 were highly variable (Todd Marks, Bureau of Land Management, written communication, 2023), ranging from almost none to nearly 0.8 Mt of NaCl extracted/year (Figure 3A). There was over twice as much annual average extracted mass in the 1996–2006 period (0.40 Mt/year) than in the 2013–2023 period (0.16 Mt/year). During at least the last part of the 1996–2023 period, the northern part of the extraction ditches was inactive (Figure 1B; potash mine personnel, verbal communication, 2022). Examination of the ratio of total KCl produced from the shallow aquifer (BSF and area south of I-80) and NaCl extracted from BSF over time shows that production became less reliant on BSF after the year 2000; with an average of 10 tonnes of NaCl extracted from BSF for every ton of KCl produced by the mine before 2000, and 5.5 tonnes of NaCl extracted from BSF for every ton of KCl produced afterward.

While seasonal precipitation and evaporation changes can impact the salinity of extracted brine (Figure 6), month-to-month analysis of density and extracted brine volumes show a clear decrease in extracted brine salinity with increased extraction rates (Figure 3D). The decrease in salinity with increased extraction suggests that deeper, less-saline waters rise upward (with reduced hydrostatic pressure) and contribute to the shallow aquifer.

From 2000 to 2004, the density of the extracted brine increased while the volume of brine extracted remained constant. From 2004 to 2015 the extracted brine density decreased; from 2004 to 2010 there was no net addition of NaCl to the salt flats. Following 2010, brine extraction greatly decreased, while laydown increased, leading to increased net volumes of brine contributed to BSF. Apparently, a 5-year lag occurred between decreased extraction with increased net brine contributions and the onset of salinity in-

crease within the system. This is a much longer period than the salinity recovery period in the early 2000s, which was associated with a much larger pulse of input solutes over a shorter period. Following increasing density up to 2015, density remained high during the 2016–2020 period.

East of Ditches and I-80 South

Both the east of ditches and I-80 south areas have reduced hydraulic connection with the halite nucleus and are isolated from laydown brines. Furthermore, brine extraction ditches impact both of these areas. Accordingly, these areas provide an example of how the brine system may respond to extraction on decadal timescales without external solute sources.

In contrast to the halite nucleus and TZE shallow aquifers, brine samples from the east of ditches and I-80 south shallow aquifers show decreases in density across individual wells and in aggregate (Figures 8A and 9). Similar to the halite nucleus crust aquifer and TZE shallow aquifer, calcium concentrations in the east of ditches shallow aquifer decreased until the 1991–1997 period (from ~1500 to 1100 mg/L) and increased afterward (to ~1400 mg/L) (Figure S4).

DISCUSSION

Brine Chemistry Changes Over Time

BSF brine chemistry changes lie within three groups: 1) no change, 2) long-term decrease or increase, and 3) change in long-term trend following the 1991–1997 period. No long-term changes in the deep and moderate-depth aquifers underlying the halite nucleus and TZE were observed. Similarly, the inner TZW area, when taken in aggregate, did not show any change in density over time. However, analyses of several wells from the TZW area indicate parts of this area increased in density over time.

The shallow aquifer in the east of ditches and I-80 south areas show clear decreases in density over time, in contrast, the outer TZW area is the only shallow brine area to show long-term increases in density across several studies. The BW production well area in the TZW also shows consistent long-term increases in alluvial-fan aquifer density, but the east of ditches and I-80 south areas show long-term decreases in brine density, with the I-80 south area showing the largest salinity decrease. The changes in brine salinity in the I-80 south area also suggest that there is limited transport of solutes under I-80 from BSF to the I-80 south area. High connectivity between these areas would likely limit salinity decreases in the I-80 south

area as transported salt would replenish removed solutes.

The last group of chemical change, with changes in long-term trends after the 1991–1997 period, indicates a change in saline pan conditions. Long-term density decreases ceased and salinity increased after the 1991–1997 period in the halite nucleus and TZE shallow aquifer (Figure 9A). On smaller timescales, brine extracted for potash production shows an increase in salinity following the onset of the laydown in 1998. Later, an increase in salinity occurred when brine extraction greatly decreased as the laydown continued (Figure 3A to C).

The onset of the laydown coincides with a marked decrease in alluvial-aquifer groundwater levels. Declining levels, in turn, reversed hydraulic gradients, enabling basinal brine movement away from the saline pan (as seen in density and isotopic changes) (Figure 16). Careful consideration of the underlying forces driving changes in brine chemistry, primarily density and water stable isotopes (e.g., laydown, decrease in brine extraction, or long-term groundwater consumption trends), is needed to identify the core controls on change that will influence management decisions.

Potential Controls on Brine Chemistry Change

Laydown

A cessation in long-term density decreases and an increase in density in the halite nucleus and TZE shallow aquifers that is concurrent with the laydown was observed. Similarly, extracted brines for potash production showed increased density in the 3- to 5-year period after the laydown began. These observations support White's (2004) hypothesis that the laydown failed to lead to a 4–5 cm increase in halite thickness because it buffered salinity decreases in the shallow brine aquifer. Although increases in aquifer density are concurrent with the onset of the laydown, changing potash brine extraction rates may have had a larger impact on observed changes in groundwater density than the laydown.

An δ^2H isotopic lightening in both halite nucleus crust brines and shallow aquifer waters over time was observed; in the absence of other information, this lightening could be attributed to isotopically lighter laydown waters. However, isotopic measurements from the east of ditches area (which is isolated from
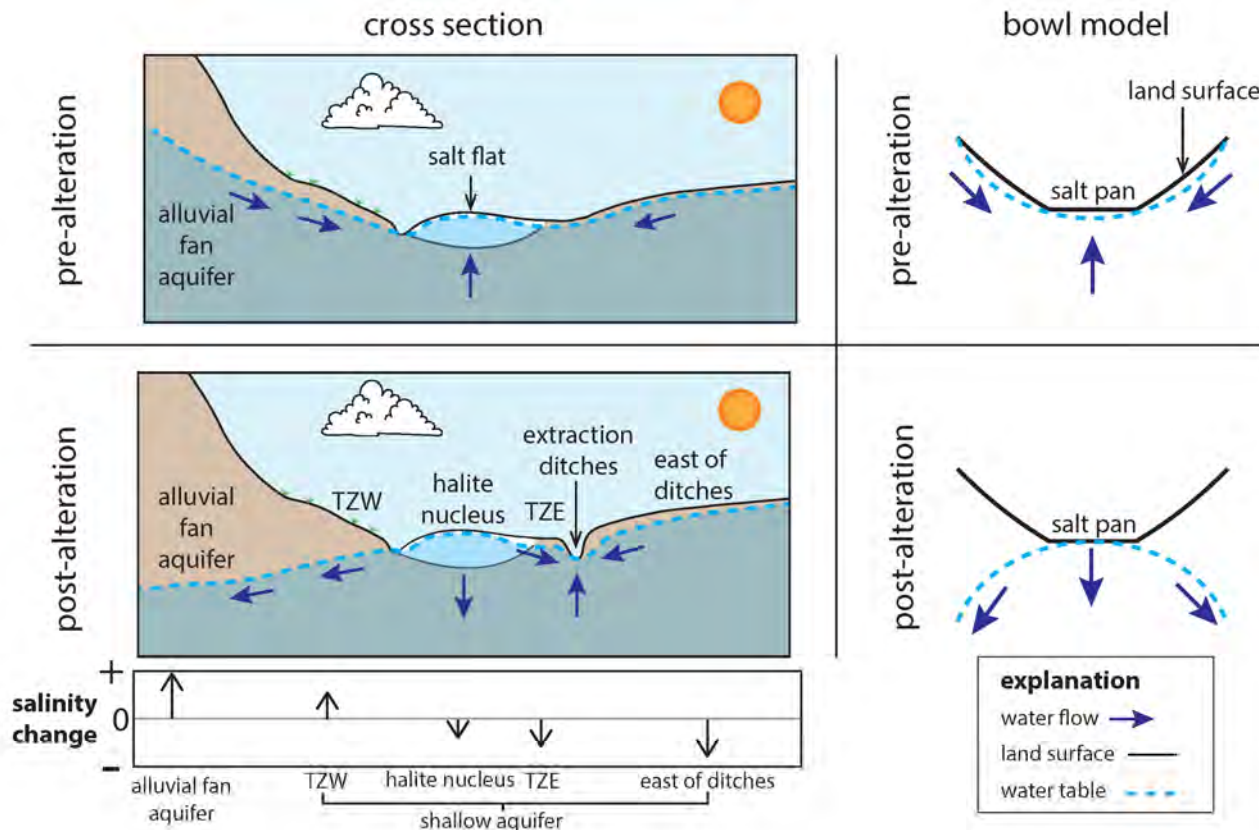

Figure 16. *Conceptual model for pre-alteration and modern groundwater (and brine) movement at BSF shown in cross section (left) and as a simplified conceptual model (right).*

laydown waters) show the same lightening over time. Therefore, a different mechanism, possibly increased infiltration of meteoric precipitation, may explain observed changes.

Changing Brine Extraction Rates

BSF brine extraction volumes before 1995 are poorly reported, leading to high uncertainty in estimated extraction volumes (Figure 9B). The average extraction volumes during the 1964–1972 and 1975–1981 periods may have been similar to or higher than those reported between 1995 and 1998. Measurements from 1999 to 2023 show stabilizing to increasing density in the halite nucleus and TZE shallow aquifers. There is a corresponding decrease in brine extraction during this period, with the largest increase in the halite nucleus shallow aquifer salinity corresponding to the greatest decrease in extraction rates. This relationship suggests that reduced extraction rates may contribute to some (and possibly most) of the observed density increases in these areas.

Examination of increasing sulfate concentrations over time relative to decreasing density in the halite nucleus and I-80 south areas shallow aquifers indicates these two values are related (Figures 9 and S7). This relationship suggests a mechanism for brine replacement after extraction. The moderate depth aquifer has elevated sulfate concentrations. When groundwater is extracted for mining, it lowers the constraining hydrostatic pressure, enabling deeper, less saline groundwater with higher sulfate concentrations to rise and replace extracted waters.

There is a positive correlation between extracted brine density and potash production brine extraction volumes (Figure 3D). Using that relationship, anticipated changes in density based on extracted brine volumes over time were modeled. While not reflecting observed density measurements (modeled density of 1.10 to 1.15 g/cm^3 between 2002 and 2010, when observed density was ~1.17 to 1.21 g/cm^3), modeled density did replicate trends in brine density change for some periods. The model replicates observed trends between 2002 and 2006 where it shows increasing and then decreasing density; it also shows increasing and then stabilized density between 2015 and 2021. Modeled and observed trends strongly differ between 2006 and 2015, where the model shows generally increasing density, while observations show generally decreasing density. These differences between observations and modeled changes suggest 1) extracted brine density may respond non-linearly to extraction rates (and accordingly, there is a lower limit for extracted brine salinity, potentially buffered from the dissolution of the halite crust); and possibly

2) under normal operating conditions (with some extraction and laydown volume of ~0.5 Mt NaCl/year) extracted brine salinity (and aquifer salinity) will decrease; additionally, 3) the large initial laydown pulse between 1998 and 2000 increased the salinity of extracted brines beyond their anticipated baseline.

Brine extraction can also depress local groundwater levels (Turk, 1973). These declines may enable infiltration of surface waters into the subsurface before they can evaporate. Isotopic lightening of the shallow aquifer (Figure 11A) may be attributed to the incorporation of isotopically lighter winter precipitation into the aquifer before significant evaporation occurred.

Given these observations, especially that changes in salinity can be attributed to extraction rates, the relative role of the laydown in increasing TZE and the halite nucleus shallow aquifer salinity remains unclear. It may be that a solute source (such as a halite crust or laydown brines) is necessary for density values to recover. Recent work on the sedimentology of BSF salt crusts documented extensive evidence of halite dissolution, suggesting that the diminishing crust is a likely source of these solutes (Bernau and Bowen, 2021).

Declining TZW Groundwater Levels

Two areas of increasing salinity were identified in the inner TZW shallow aquifer, and a long-term aggregate trend in increasing salinity in the outer TZW shallow aquifer was also found. Kipnis (2021) and Lines (1979) noted decreasing groundwater levels in these areas. Furthermore, several dry outer TZW shallow wells were noted during this investigation. Two mechanisms for increasing TZW shallow aquifer salinity are proposed: 1) the TZW inner area receives brine from the halite nucleus aquifers and surface precipitation, and 2) salinity that was once concentrated at the surface by efflorescence and then recycled basinward now accumulates in groundwater as the capillary fringe falls below the ground surface. Flow of halite nucleus brine to the inner TZW area may be enhanced by declining TZW hydraulic head. Furthermore, there is the potential for laydown brines (which accumulate on the western halite nucleus edge) to enter the TZW area.

Several observations, such as declining western halite nucleus shallow aquifer salinity and areas of inner TZW with increasing salinity, support the interpretation that westward movement of shallow aquifer brine contributes to recent declines in BSF crust thickness. Between the 2003 and 2016 salt crust thickness studies, the area on the southwestern side of BSF had some of the largest observed decreases in salt crust thickness. This area is also the closest part

of BSF to the alluvial-fan production wells. During the same period, the northernmost parts of the BSF crust reduced in volume; those declines may be attributable to their distance from the thickest part of the halite crust.

The alluvial-fan aquifer shows several significant changes over time. The decline in groundwater levels has reversed the hydrological gradient such that basinal waters now flow toward the mountain front. The movement of basinal waters toward the mountain front is demarcated by changes in brine density and δ^2H and δ^{18}O isotopes. Formerly fresh production wells now produce waters that exceed the salinity of the ocean ($\sim$35 ppt or 1.03 g/cm^3). These changes indicate that basinal brine (possibly the halite nucleus shallow and crust aquifer brine) is being removed from the saline pan area (Figure 16). Isotopic and density data should be considered to determine the relative sourcing of waters extracted by production wells to estimate how much brine will be removed from the halite nucleus area under different alluvial-fan extraction scenarios.

Climate Does Not Explain Observed Alluvial-Fan Groundwater Level Declines

Between 1993 and 2010, there were frequent drought periods, with the majority of years experiencing precipitation levels below the 25% quartile for precipitation based on data from 1910 to 2020 (Bernau, 2022). Before the 1990s, alluvial-fan aquifer levels varied but regularly returned to the land surface. In the period since then, they have shown a clear long-term decline that strongly differs from observations of similar alluvial-fan aquifer wells in the GSLD, which have remained relatively stable to slightly increasing over this period (NWIS, https://maps.waterdata.usgs.gov/mapper/index.html, sites 404757112582701 and 394905113354101). These data indicate that recent declines in the alluvial-fan aquifer are occurring because extraction rates have exceeded recharge rates for over two decades.

Impact of Laydown on Alluvial-Fan Aquifer Drawdown

Before 1997, the alluvial-fan groundwater level remained within 0 to 7 m of the surface (Kipnis and Bowen, 2018; Mason and Kipp, 1998). Following the laydown, groundwater levels never rose above 10 m below ground level and have continued to decline (Figure 3E). This suggests that groundwater levels have not yet reached a new equilibrium where inflow is equal to pumping rates and a larger area will be drained over time. The relative proportion of basinal water in produced alluvial aquifer waters will increase as this area expands. The laydown has led to as much as a doubling in alluvial groundwater extraction, and as such, plays a major role in decreasing alluvial-fan groundwater levels.

CONCLUSIONS

New chemical and groundwater level measurements and past research were compiled to examine multi-decadal changes at the Bonneville Salt Flats. Brine chemistry, most notably density and δ^2H and δ^{18}O water isotopes, has changed in response to anthropogenic activities (Figure 16). Shallow aquifer brine under and to the east of the crust declined in salinity between 1964 and 1997 and stabilized and increased in salinity afterward. Increased salinity may be due to decreased extraction rates in the past two decades, especially as the largest increase in salinity, during the 2013–2023 period, is concurrent with the largest decrease in extraction. However, this period is also concurrent with the experimental salt restoration laydown program. The relative role of the laydown in increasing aquifer salinity remains unclear. Alluvial aquifer groundwater levels have declined over time. This decline is linked to industrial water production, including the laydown. As a result, the hydraulic gradient has reversed, causing brine to flow away from the saline pan and towards the alluvial aquifer. This flow increases alluvial fan aquifer salinity and changes its isotopic composition. If alluvial-fan extraction rates remain the same, or if they rise with increases to the laydown, more salt will be removed from the Bonneville Salt Flats halite nucleus, potentially at volumes exceeding the laydown. These multi-decadal chemical changes inform the understanding of groundwater movement and halite crust changes in this system, which informs management for the sustained use of this landscape.

Supplemental Data

Supplemental data and figures are available at https://doi.org/10.5281/zenodo.8152647.

ACKNOWLEDGMENTS

REFERENCES

Agapito Associates, Inc., 2022, Technical Report Summary of 2021 Estimated Resources and Reserves at Intrepid Potash-Wendover, 262 p.

Bernau, J.A., 2022, Spatial and temporal scales of water and salt movement at the Bonneville Salt Flats: Salt Lake City, University of Utah, Ph.D. dissertation, 195 p.

Bernau, J.A., and Bowen, B.B., 2021, Depositional and early diagenetic characteristics of modern saline pan deposits at the Bonneville Salt Flats, Utah, USA: Sedimentology, p. sed.12861.

Bernau, J.A., Jagniecki, E.A., Kipnis, E.L., and Bowen, B.B., 2023a, Applications and limitations of portable density meter measurements of Na-Ca-Mg-K-Cl-SO$_4$ brines: Chemical Geology, v. 616, p.121240

Bernau, J.A., Oviatt, C.G., Clark, D.L. and Bowen, B.B., 2023b, Sediment logs compiled from the Great Salt Lake Desert, western Utah, with a focus on the Bonneville Salt Flats area: Utah Geological Survey Open-File Report 754, 24 p., 3 appendices, https://doi.org/10.34191/OFR-754.

Bethke, C.M., 2013, Geochemical and biogeochemical reaction modeling: Cambridge University Press, Cambridge, UK, p.1689–1699.

Bingham, C.P., 1980, Solar production of potash from the brines of the Bonneville Salt Flats: Utah Geological and Mineral Survey Bulletin, v. 116.

Bowen, B.B., Kipnis, E.L., and Pechmann, J.M., 2018, Observations of salt crust thickness change at the Bonneville Salt Flats from 2003-2016, *in* Emerman, S.H., Bowen, B.B., Simmons, S., and Schamel, S. editors, Geofluids of Utah: Utah Geological Association Publication 47, p. 247–285.

Bowen, B.B., Kipnis, E.L., and Raming, L.W., 2017, Temporal dynamics of flooding, evaporation, and desiccation cycles and observations of salt crust area change at the Bonneville Salt Flats, Utah: Geomorphology, v. 299, p. 1–11.

Dansgaard, W., 1964, Stable isotopes in precipitation: Tellus, v. 16, no. 4, p. 436–468.

Hadzeriga, P., 1964, Some aspects of the physical chemistry of potash recovery by solar evaporation of brines: Society of Mining Engineers, v. 013, p. 169–174.

Harvie, C.E., Moller, N., and Weare, J.H., 1980, The prediction of mineral solubilities in natural waters—the Na-K-Mg-Ca-Cl-SO$_4$-H$_2$O system from zero to high concentration at 25°C: Geochimica et Cosmochimica Acta, v. 44, no. 7, p. 981–997.

Hipel, K.W., and McLeod, A.I., 1994, Time series modelling of water resources and environmental systems: Elsevier Science, Amsterdam, Netherlands.

Kipnis, E.L., 2021, Geologic change, hydrologic drivers, and resource use at the Bonneville Salt Flats, Utah, USA: Salt Lake City, University of Utah, Ph.D. dissertation, 100 p., 2 appendices.

Kipnis, E.L., and Bowen, B.B., 2018, Observations of salt crust change from 1960-2016 and the role of humans as geologic agents at the Bonneville Salt Flats, Utah, *in* Emerman, S.H., Bowen, B.B., Simmons, S., and Schamel, S. editors, Geofluids of Utah: Utah Geological Association Publication 47, p. 287–303.

Kipnis, E.L., Bowen, B.B., Hutchings, S.J., Hynek, S.A., and Benison, K.C., 2020, Major ion geochemistry in Na-Ca-Mg-K-Cl-SO$_4$ brines using portable X-ray fluorescence spectrometry: Chemical Geology, v. 558, no. September, p. 119865.

Lerback, J.C., Hynek, S.A., Bowen, B.B., Bradbury, C.D., Solomon, D.K., and Fernandez, D.P., 2019, Springwater provenance and flowpath evaluation in Blue Lake, Bonneville basin, Utah: Chemical Geology, v. 529, no. April, p. 119280.

Lindenburg, G.J., 1974, Factors contributing to the variance in the brines of the Great Salt Lake Desert and the Great Salt Lake: Salt Lake City, University of Utah, M.S. thesis, 70 p.

Lines, G.C., 1978, Selected ground-water data, Bonneville Salt Flats and Pilot Valley, western Utah: U.S. Geological Survey Utah Basin-Data Release, no. 30, 14 p.

Lines, G.C., 1979, Hydrology and surface morphology of the Bonneville Salt Flats and Pilot Valley playa, Utah: U.S. Geological Survey Geological

Survey Water-Supply, v. 2057, no. 2057, p. 1–107.

Mason, J.L., Brothers, W.C., Gerner, L.J., and Muir, P.S., 1995, Selected hydrologic data for the Bonneville Salt Flats and Pilot Valley, western Utah, 1991-93: U.S. Geological Survey Open-File Report, v. 95–104, p. 1–56.

Mason, J.L., and Kipp, K.L., 1998, Hydrology of the Bonneville Salt Flats, northwestern Utah, and simulation of ground-water flow and solute transport in the shallow-brine aquifer: U.S. Geological Survey Professional Paper, v. 1585, p. 108.

McLeod, A.I., 2022, Kendall Rank Correlation and Mann-Kendall Trend Test. R code

Munk, L.A., Boutt, D.F., Moran, B.J., McKnight, S.V., and Jenckes, J., 2021, Hydrogeologic and geochemical distinctions in freshwater-brine systems of an Andean salar: Geochemistry, Geophysics, Geosystems. v. 22, no. 3, 20 p. https://doi.org/10.1029/2020GC009345

Nolan, T.B., 1927, Potash brines in the Great Salt Lake Desert, Utah, Chapter B, *in* Contributions to economic geology (short papers and preliminary reports): U.S. Government Printing Office, p. 25–44.

Oviatt, C.G., Clark, D.L., Bernau, J.A., and Bowen, B.B., 2020, Data on the surficial deposits of the Great Salt Lake Desert, Bonneville Salt Flats and east part of the Wendover 30' x 60' quadrangles, Tooele County, Utah: Utah Geological Survey Open-File Report, 70 p.

Penrod, C.L., 2016, The geochemistry of meteoric water and surface-pond brines at Bonneville Salt Flats, UT: Salt Lake City, University of Utah, M.S. thesis, 30 p.

Pitzer, K.S., 1973, Thermodynamics of electrolytes–I—Theoretical basis and general equations: Journal of Physical Chemistry, v. 77, no. 2, p. 268–277.

Plummer, L.N., Parkhurst, D.L., Fleming, G.W., and Dunkle, S.A, 1988, A computer program incorporating Pitzer's equations for calculation of geochemical reactions in brines: U.S. Geological Survey, Water-Resources Investigations Report, v. 88–4153, p. 707–720.

Post, V., Kooi, H., and Simmons, C., 2007, Using hydraulic head measurements in variable-density ground water flow analyses: Ground Water, v. 45, no. 6, p. 664–671.

R Core Team, 2021, R: A language and environment for statistical computing, R Foundation for Statistical Computing, Vienna, Austria. https://www.r-project.org/

Radwin, M.H., and Bowen, B.B., 2021, Mapping mineralogy in evaporite basins through time using multispectral Landsat data—Examples from the Bonneville basin, Utah, USA: Earth Surface Processes and Landforms, v. 46, no. 6, p. 1160–1176.

Read, E.K., Carr, L., De Cicco, L., Dugan, H.A., Hanson, P.C., Hart, J.A., Kreft, J., Read, J.S., and Winslow, L.A., 2017, Water quality data for national-scale aquatic research: The Water Quality Portal, Water Resources Research, v. 53, no. 2, p. 1735–1745.

Shaw Environmental, 2020, Intrepid Potash Mine and Reclamation Plan, submitted to Utah Division of Oil, Gas, and Mining: 1943 p., https://ut-dnr-ogm-prod-sf-public-bucket.s3.amazonaws.com/5624847.pdf

Shuey, R.T., 1971, Paleomagnetic chronology and correlation of Great Salt Lake basin sediments: Washington D.C., National Science Foundation, Final Technical Report for grant GA-16134, 15 p.

Soil Survey Staff, Natural Resources Conservation Service, United States Department of Agriculture, undated, Web Soil Survey. Available online: https://websoilsurvey.nrcs.usda.gov/app/WebSoilSurvey.aspx, accessed March 2023.

Stephens, J.C., 1974, Hydrologic reconnaissance of the northern Great Salt Lake Desert and summary hydrologic reconnaissance of northwestern Utah: United States Geological Survey, 55 p.

National Water Quality Monitoring Council, undated, The Water Quality Portal, https://www.waterqualitydata.us/, accessed November, 2022.

Turk, L.J., 1973, Hydrogeology of the Bonneville Salt Flats, Utah: Utah Geological and Mineral Survey, 82 p.

Turk, L.J., Davis, S.N., and Bingham, C.P., 1973, Hydrogeology of lacustrine sediments, Bonneville Salt Flats, Utah: Economic Geology, v. 68, no. 1, p. 65–78.

Utah Division of Natural Resources, undated, Water Rights database: https://www.waterrights.utah.gov/wrinfo/query.asp, accessed November, 2022.

White, W.W., 2002, Salt Laydown Project—Replenishment of Salt to the Bonneville Salt Flats, in Gwynn, J.W., editor, Great Salt Lake: An Overview of Change: Utah Geological Survey Special Publication, p. 433–486.

Wilkinson, G.N., and Rogers, C.E., 1973, Symbolic description of factorial models for analysis of variance: Journal of the Royal Statistical Society, Series C, v. 22, no. 3, p. 392–399.